Vermersch Thomas

Opoka Daniel

Podeur Emma

RETRO ENGINEERING OF AN FZG TEST RIG BENCH MODEL

Tutors Jérôme Cavoret and Valentin Ripard

Date: 25th March 2021

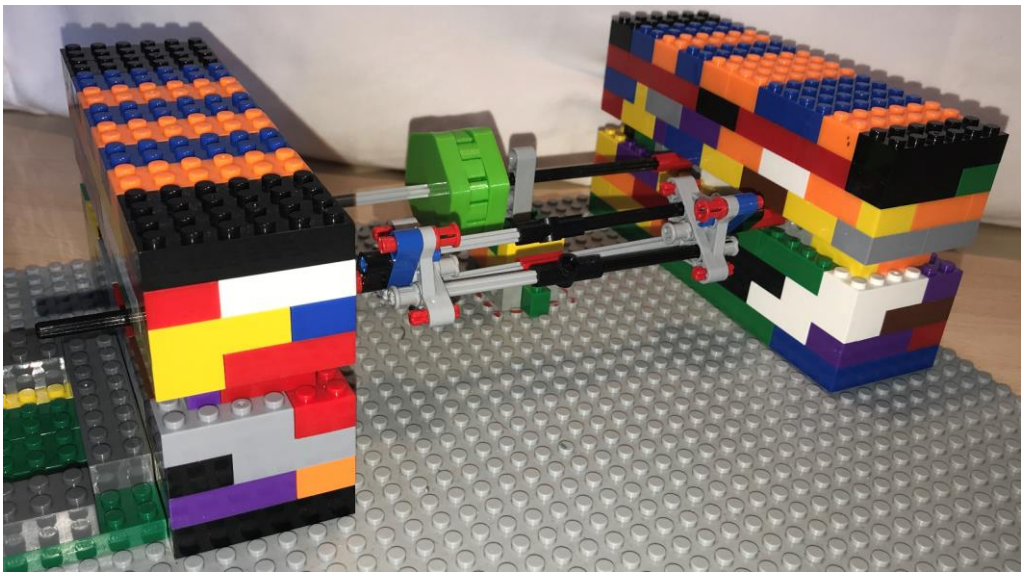

INSA INSTITUT NATIONAL DES SCIENCES APPLIQUÉES LYON

We would like to thank our tutors Jérôme Cavoret and Valentin Ripard for supporting and helping us and without whom this project would not have been able to be developed to its fullest of potential. Furthermore, we would like to acknowledge Mr. Velex for proposing and enabling us to do this project.

Table des matières

Introduction

Retro-engineering, or reverse engineering, is the process of recreating a system through deductive reasoning with the available materials given to the project. To accomplish this, first the purpose of every component must be understood so that the parameters that make it up can be recreated or re-interpreted. The goal of this re-design is to build a model that adequately represents the original system [1]. This concept is versatile and can be used in many fields of engineering, however in this report the focus is on the reconstruction of the FZG test rig with Lego pieces. One begins with a general concept of the test rig and through deduction and a firm understanding of the machine, a competent recreation can be made. After which improvements can be done on the original model. The following Figure 1 illustrates this process.

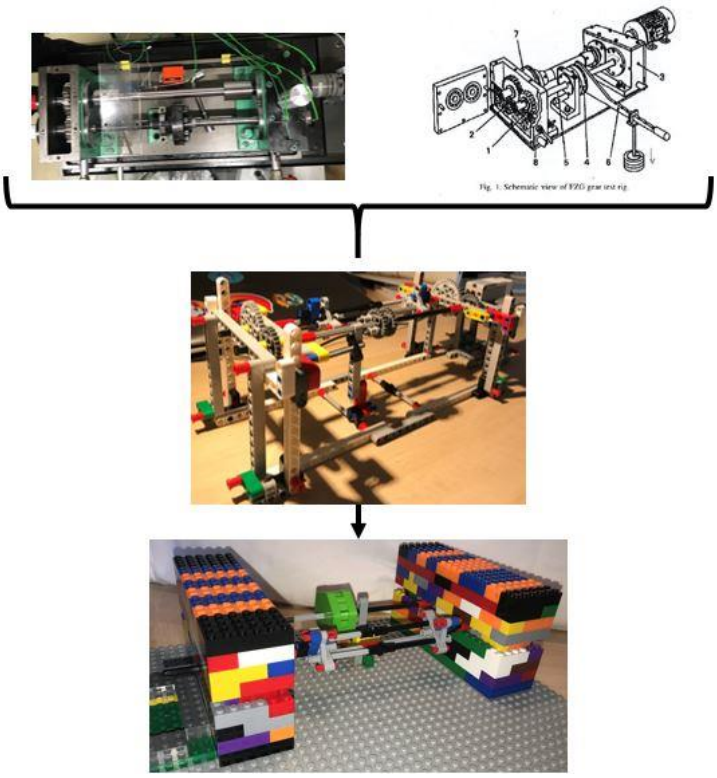

Figure 1: Illustration of Retro-Engineering

First semester's work from September 2020 to December 2020 concluded on the creation of a Lego model. It could re-enact the function of the clutch of the original FZG test rig, which is to induce a torque into the system. This would allow the study of how a pair of gears would react under such a load and/or qualify a lubricant under such conditions. Additionally, a Torsional Demonstration Shaft was created on the driving shaft to help illustrate how much torque was in the system. This model, however, had many shortcomings, one of which being that it did not distribute neither the induced torque nor the vibrations properly throughout the entire structure. Furthermore, the clutch was rudimentary and could be improved.

The work completed in the first semester has been continued with the objective of creating a more stable Lego model. Also, it was of interest to create experimental and analytical models of power loss that occurs during the operation of the Lego model. By acquiring specific Lego pieces, a sturdier structure was created, and a 3-D printed clutch was designed to allow more tests.

1. Objectives

The second part of this project aimed at developing on what was previously done in first semester. The objectives of this semester are directed towards the analytical part of the model. The main objective is to quantify the power losses of the test rig both from an analytical and experimental point of view and be able to provide a comparative analysis between both using MATLAB.

On the experimental level, many tests were performed on the Lego model test rig to estimate the power losses of the motor when it is under different configurations. A large focus was brought on remodelling the clutch system to study a greater range of torsion induction and to propose a more practical solution that better suited the Lego model. Finally, a test method to validate the results was performed using a water bottle and a string.

On the analytical level, a torsional stiffness analytical model was built to better account for the torsional effects on the shafts for use in future analytical models. The analytical model for the power losses considered the different mechanical behaviours of the Lego model, such as, the friction between the meshed gear teeth and the torsion that could be induced unto the system through the clutch. The last part was focused on observing and understanding the power losses using the vibrations generated by the Lego Model. This part was a secondary objective and was an exploration path.

2. FZG test rig

2.1 Introduction

The FZG test rig is a testing machine originally developed in the 1950's by FZG company for testing lubricants and their load carrying capacity [2]. The company is known for developing a standardized method for determining the relative scuffing load-carrying capacity of oils. Later on, the company developed standard testing for extreme pressure (EP) oils and semifluid gear greases [2]. Nowadays, it is unthinkable to develop any lubricant without submitting it to these standardized tests. In order to carry out the tests, a back-to-back test rig system was designed for testing lubricants at low to medium rotational speeds (1500- 20000 rpm). To certify a lubricant, it is submitted to a series of processes that use different rotational speeds and set the oil to a certain temperature. Many countries use the system of the International Standardized Organization Viscosity Grade (ISO VG) [3] to quantify oils by their viscosity is one of the main criteria of selection for lubrication oils. Other countries use the American Petroleum Institute criteria (API G1 to G5) [4] [5]). In the case of the FZG, it is used to test scuffing and micro-pitting [6]. Any lubricant that wants to be commercialised has to be qualified by passing these standardized tests before commercializing the product.

2.2. FZG test rig description

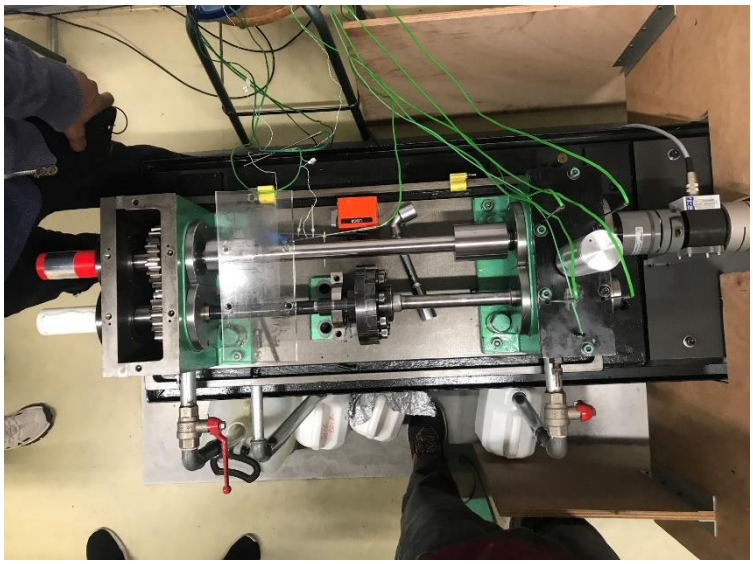

Figure 2: Top view perspective of FZG test rig

To have a better understanding of the test rig system, a detailed explanation will be provided on the different components that make it up. The FZG test rig can be observed on Figure 2. It is a four-gear mechanism that is composed of a test box and a slave box, and each gearbox houses a pair of pinion and driven gear where both are spur gears. Shafts connect the two gearboxes. The first shaft is equipped with a clutch system to induce torque; therefore, the transmission creates a mechanical loop. This is performed to simulate the real conditions that the mechanical system can be subjected to [7].

2.2.1. Shafts description

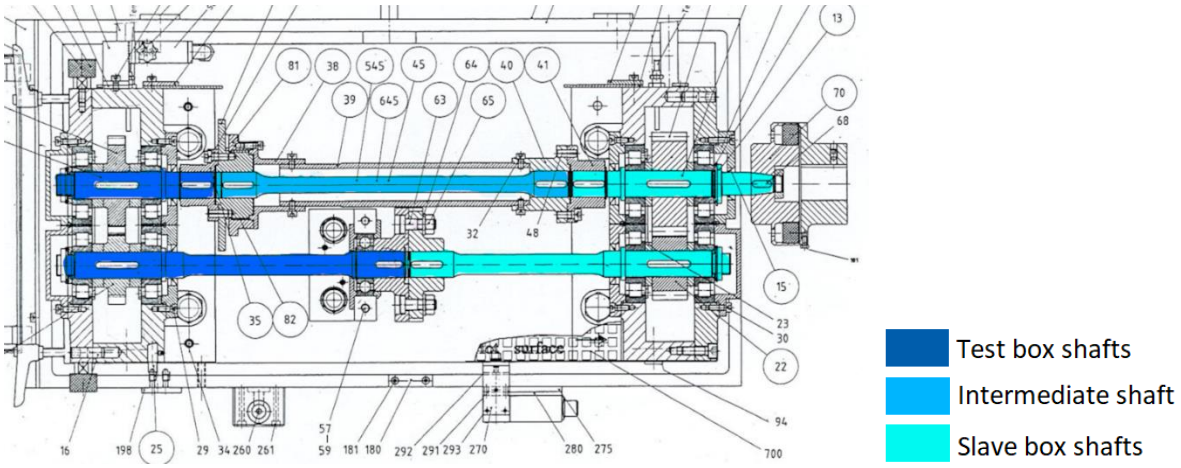

Figure 3: Schematic drawing with shafts highlighted

As Figure 3 presents, the bottom shaft is composed of two shafts being the test box shaft and the slave box shaft. Both shafts are connected by the clutch mechanism. In the case of the upper shaft, there is a system of three shafts. Two of the shafts are coupled to the pinion gears and an intermediate shaft links both. This was done to allow easier access when assembling and disassembling the rig. The slots on both shafts are made for the keys to attach the pinion and the gear on the shaft, this is done for practical purposes to be able to switch gears easily. The gears elements have a cut- out for the key so that the torque can be transmitted and thus rotation induced.

2.2.2. Gearboxes description

The gears in both gearboxes are mounted in the same way. The diagram in Figure 4, shows the pinions and gears highlighted in magenta and purple respectively. Each gear element is placed between two sets of bearings represented in yellow and spaced out with spacers. Bearings are used to reduce the friction between the shafts and housing while the reason for using spacers is to avoid any possible contact between the bearing and gear element which could damage either parts.

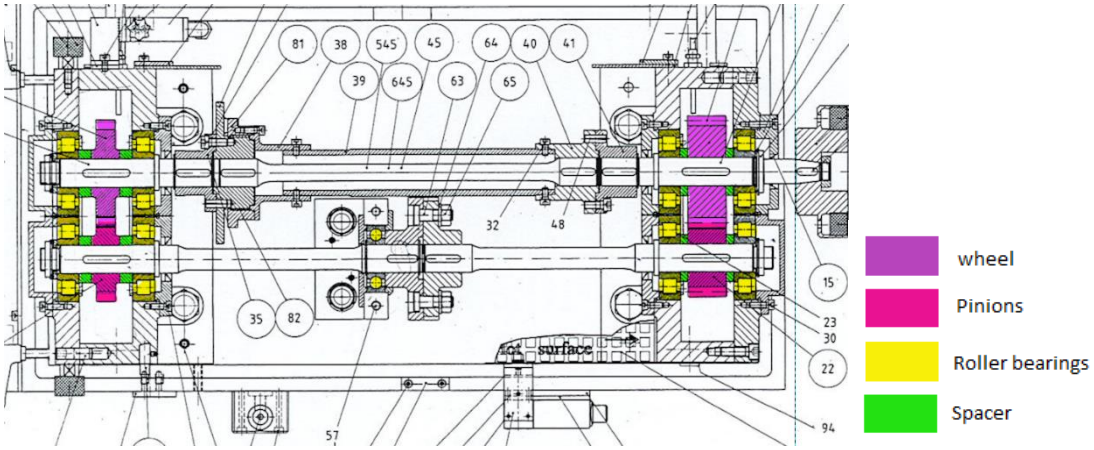

Figure 4: Schematic drawing with gears and bearings highlighted

2.2.3. Clutch mechanism

The clutch mechanism is an essential component of the test rig. As previously mentioned, it allows to introduce torque into the system, and simulate the forces that the pinion and wheel are exposed to when in operation in a mechanical system. As a result, this induces a torsion in all the shafts of the test rig and generates large amounts of pressure on the teeth of the wheel and pinions. This mechanism is built with two main parts, the right and left clutch pad that are highlighted in different colours in Figure 5.

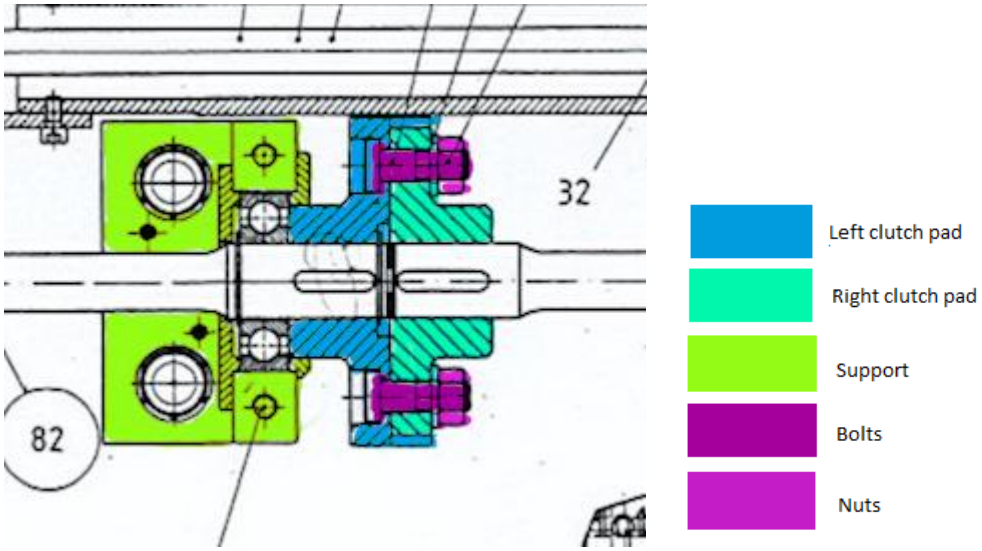

Figure 5: Schematic top view drawing of the clutch mechanism

The bolts are inserted through the left clutch via an opening that can rotate to allow insertion of all the bolts. On the right-hand side of Figure 6, nuts (in purple) are used to tighten both parts together. When a new load needs to be applied, the bolts and nuts are simply untightened and not entirely removed.

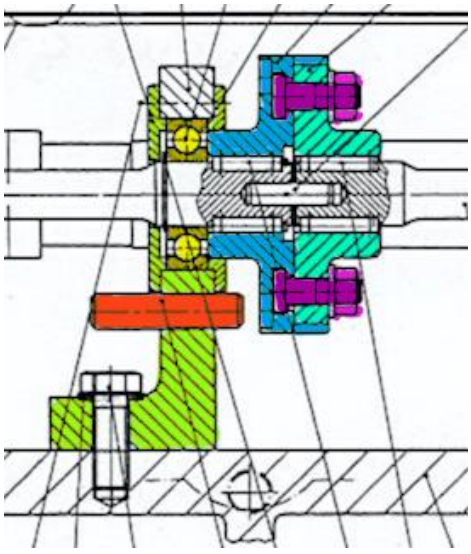

Figure 6: Schematic side view drawing of the clutch mechanism

The shafts are interconnected via the gears, hence there needs to be a solution to maintain one of the shafts fixed while a torque is being applied. This is why a key is used (designated in orange) which is inserted in a slot on the left clutch pad and locks it into position. As the shaft is submitted to large forces when applying a torque, a support represented in green, prevents the centreline of the shaft from becoming misaligned. A picture of the actual key and slot can be found in Annexe 1.

2.2.4. Clutch CAD Model

The following CAD model proposed for the clutch is based on the interpretation and schematics of the clutch mechanism. The casing that is mounted on the left clutch pad is not represented to be able to clearly see the internal design of the clutch.

Figure 7: Clutch CAD model

As previously mentioned, the slot for the key in Figure 8 is located on the casing of the left clutch pad. On the right clutch pad there are hinges where a lever can hook onto to easily introduce torque into the system. The nature of the oblong wholes on the left clutch pad are there to allow for a degree of freedom for the bolts when the right clutch pad is rotated. As can be seen in Figures 7 and 8, the hinges on the right clutch pad are there so that a lever can hook onto and introduce torque much easier

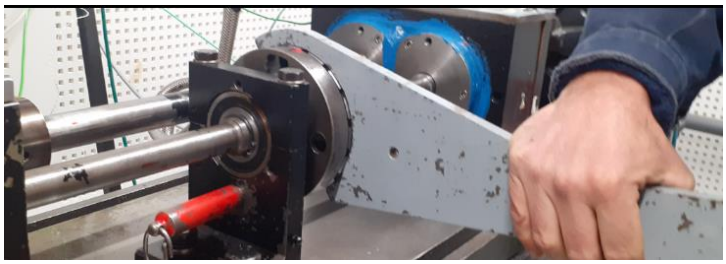

Figure 8: Picture of the Clutch mechanism when torque is being applied

2.3. Loading procedure of the test rig

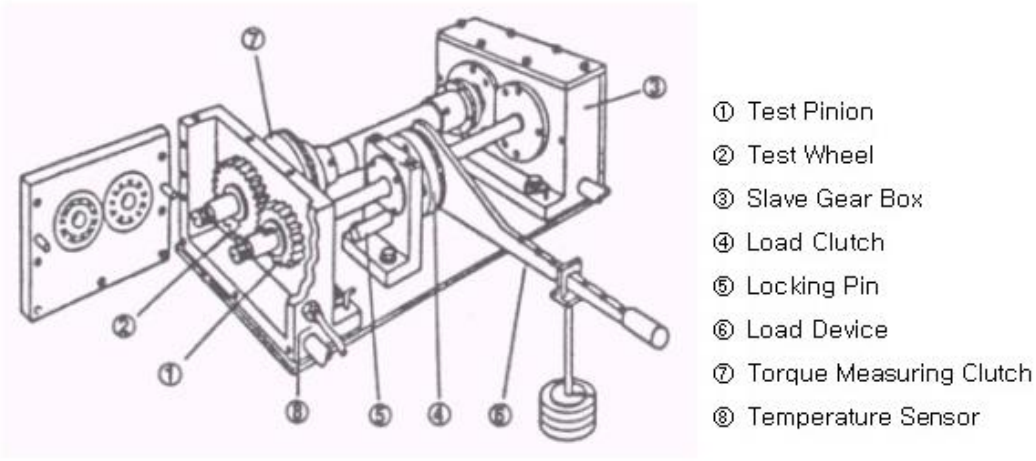

Figure 9: Technical drawing of the FZG test rig with the load device [8]

These are the steps followed to induce a torque into the system before it is run.

1. To apply a load, the nuts must be loosened to free the contact between both clutch pads.
2. The left clutch pad is locked into place by inserting the key through the hole of the bearing support to the left clutch pad.
3. A torque is induced using a lever where a varying amount of weight can be placed at a known distance on the arm.
4. Whilst maintaining that load, the nuts are fastened tightly to keep the torque in the system.
5. The load device and the key can both be removed, after which the system is closed, and it can be run [7]

3. Lego model

3.1. General Description

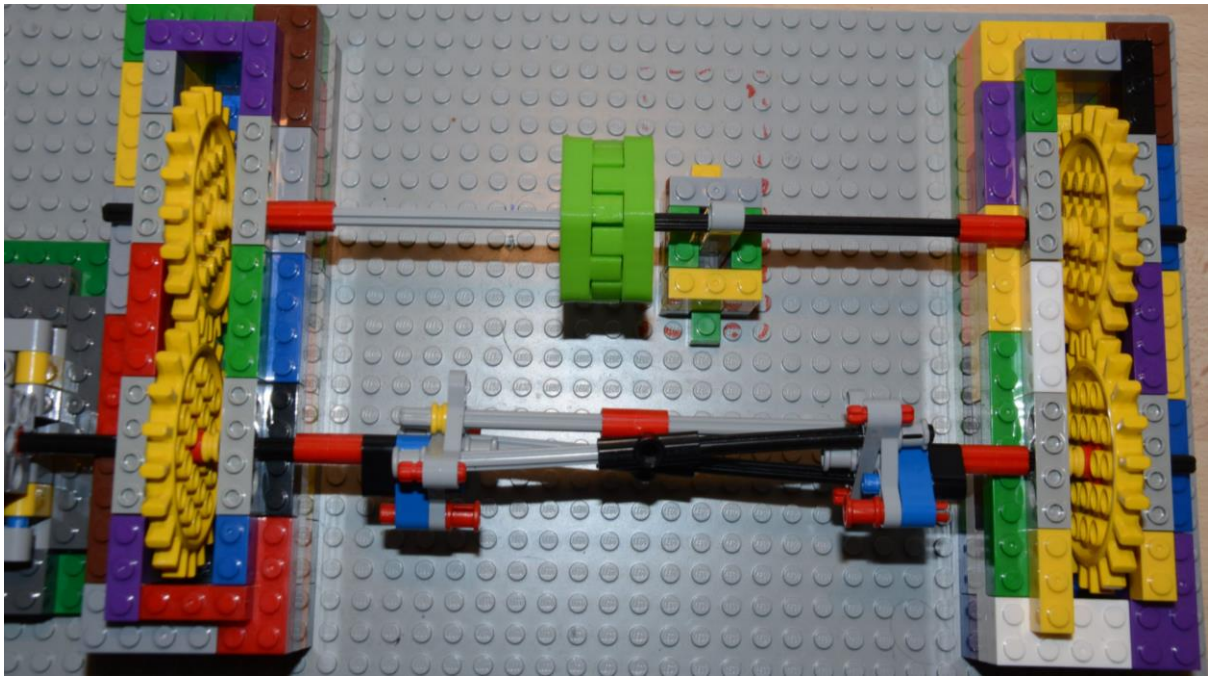

Figure 10: Final Lego Model

Many improvements were made between last semester model and the final model presented today. The main objectives of this semester were to create a close replica of the actual FZG test rig as well as reducing the vibrations generated by the system. To reduce the vibrations, a baseplate of 48x48 cm was placed so that the motor and the test rig could be more stable and attached to the same base.

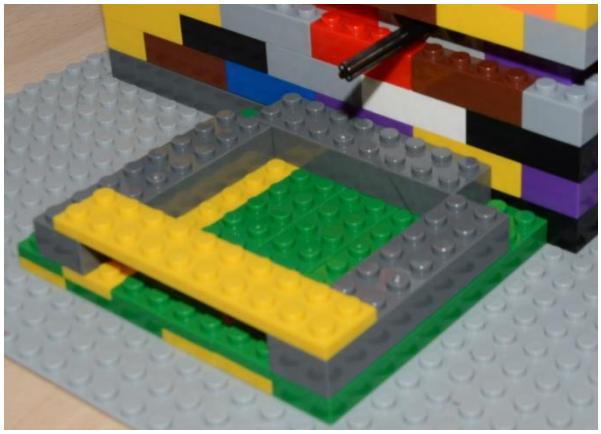

Figure 11: Motor stand

A stand was built to fix the motor and to align it to the shaft, shown in Figure 11. Additionally, instead of having a frail structure to support the gears and the shafts, two casing in Figure 10 were made to replicate the effect of the gearboxes in the actual FZG test rig: the gearbox that runs the system is called the master gearbox (closest to the motor), the other one is called the test gearbox. Each Lego bricks layer is laid offset from the previous one to enhance the stability of the walls/casings.

On the other hand, the Torsional Demonstration shaft and the other five shafts were similar to the model used for the previous semester in order to represent effectively the torsion inside the shafts when torque is applied, as can be observed in Figure 12.

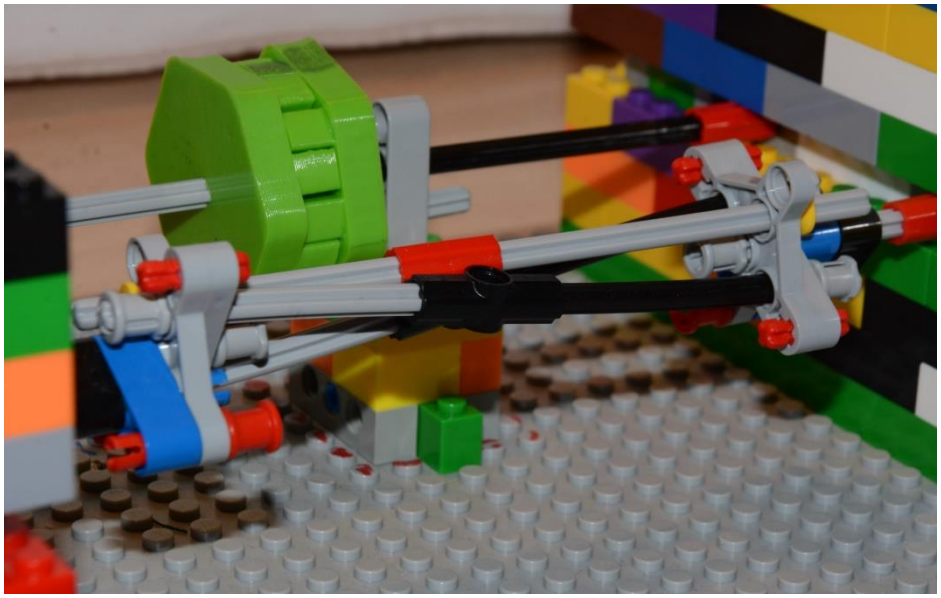

Figure 12: Zoom in of the 3-demonstration shafts

3.1. 3-D printed clutch

From the Lego model of the previous semester, two gears were used to apply a certain amount of torque. However only three tests could be recorded by twisting the right part of the gear starting from 0°, then 90° and 180°. To expand the number of torque applied up to five, it was decided that another clutch model would be 3-D printed.

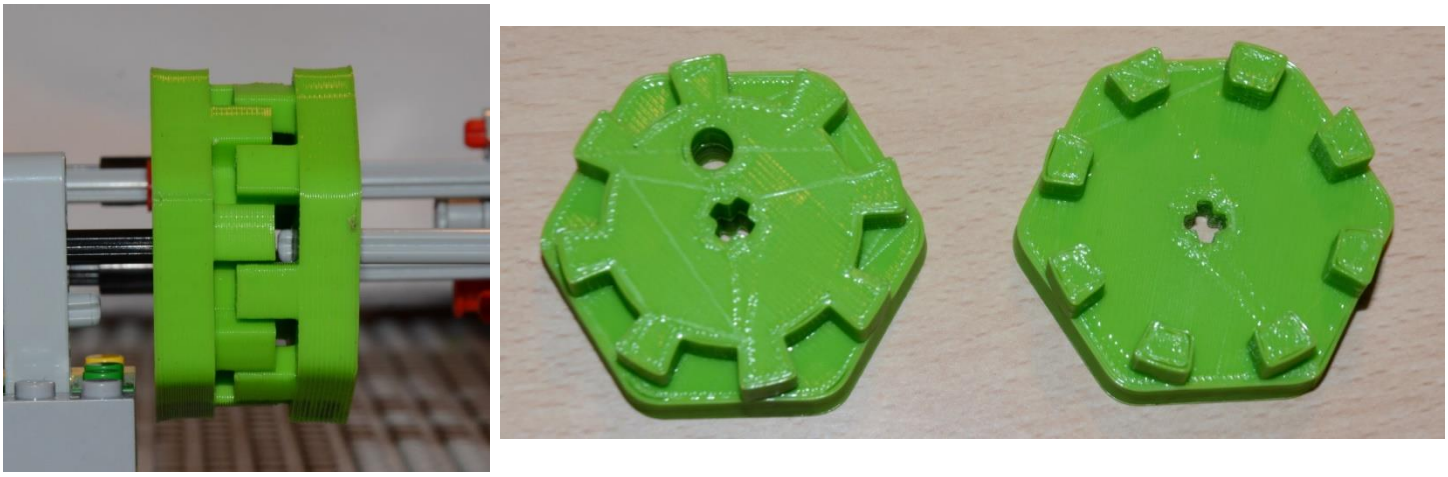

Figure 13: Clutch Mechanism

As can be seen on Figure 13, the 3-D printed clutch is made of an interlocking mechanism made of two parts: the left one is kept in place by inserting a shaft into the small hole, while the right part is twisted at a certain degree defined by the teeth fitting into the left part holes. This mechanism allowed us to discard the two shafts used to hold the torque in the previous model. Moreover, it was possible to record five different tests: 0°, 45°, 90°, 135° and 180°. For this purpose, the diameter of the part had to be increased. The conception of the clutch was not only focused on increasing the number of angles of torque, but also on making the clutch more practical. Thus, the sides were drawn flat so that it is more convenient to apply torque and fillets were added on the six edges of the hexagon to eliminate any sharp edges that can be easily damaged, or that could cause injury when the part is handled.

3.2. Gears

The initial goal was to replicate the teeth ratio of the actual test rig 16/24, however keeping in mind that the main objective was to make the Lego casings as large as possible, four gears of the same dimensions were used because they were the largest ones available.

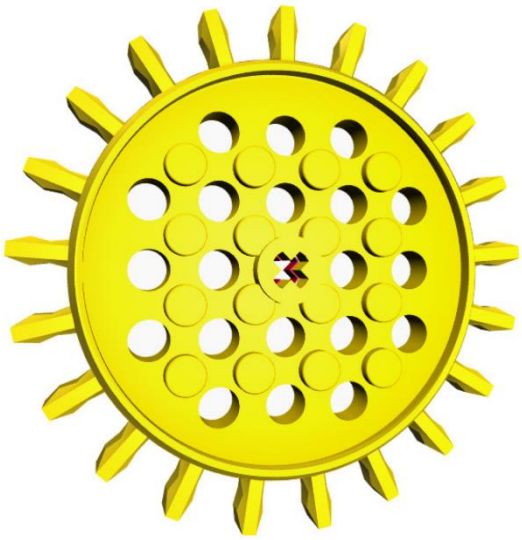

Figure 14: Lego Gear used for the final model

No information was given about the gears except for its number of teeth, therefore mounting hole, pitch radius, tooth thickness and centre distance had to calculated using a calliper. Pressure angle was estimated to be 20°. Table 1 represents the gear parameters:

Table 1: Gear parameters

	Pinion	Gear
mounting hole (cross section)	L=1.85mm l=4.8mm	L=1.85mm l=4.8mm
r_a: outside radius	5.75mm	5.75mm
m_0: module	0.5mm	0.5mm
a: centre distance	55.5mm	
z: number of teeth	21	21
α: angle of pressure	20	
b: face width	0.8cm	0.8cm
x: Profile shift coefficient	0	0
h_a: tooth addendum	0.5mm	0.5mm
h_b: tooth dedendum	0.625mm	0.625mm
p_b: base pitch	1.3838	1.3838

Calculations of the parameters can be found in Annexe 2.
The properties of the gears will be used in the calculation of the Power Losses section.

3.3. Kinematic diagram

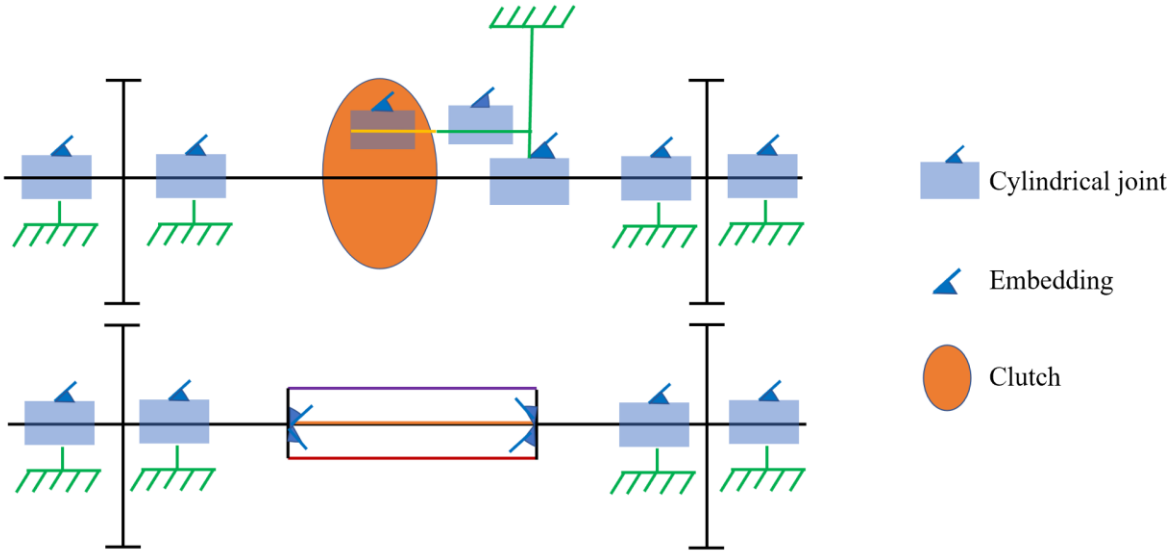

Figure 15: Kinematic diagram locked system

To apply a certain amount of torque, one part of the clutch (further to the motor) had to be locked into place by sliding one shaft through two cylindrical joints as seen in Figure 15.
The Torsion Demonstrational shaft is represented with embedded connections as the joints allow the three shafts to rotate together in order to represent one object. The two pinions and the two gears are fixed by cylindrical joints so that alignment is insured.

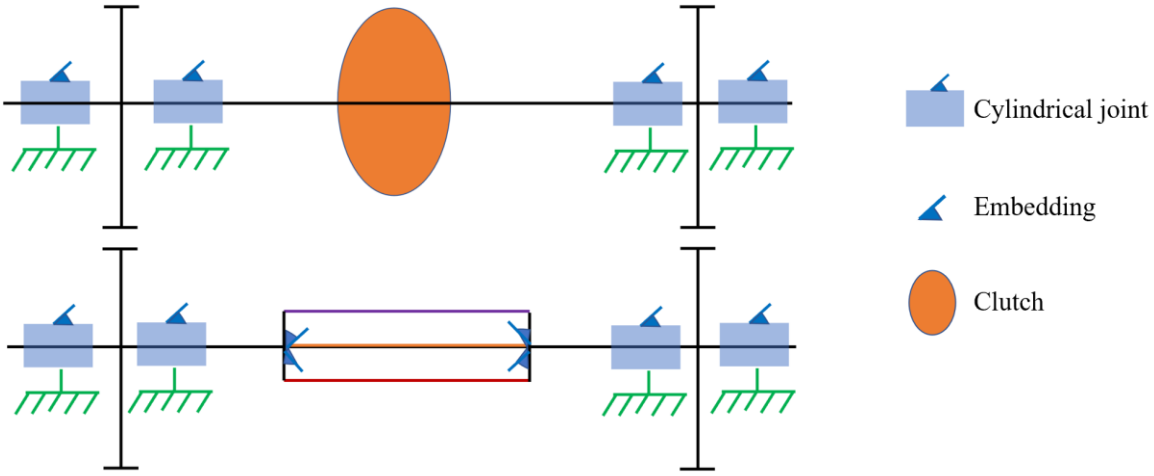

Figure 16: Kinematic diagram non-locked system

Once the torque is applied, the connection shaft used to hold in place the clutch is removed. The system is now connected and the mechanical transmission is being transmitted through the clutch.

4. Experiments and modelling

4.1. Torsional stiffness test and analytical model

4.1.1. Experiment

The shaft was clamped by a stand made of Lego pieces. The rotating stand had a lever mechanism to apply a moment on the structure of the shaft being tested (represented in orange in Figure 17). By hanging a mass, the model's ability to resist when moments apply was measured. This process was repeated for different masses, for which the angle between the lever (represented in purple in Figure 17) and the horizontal axis was measured.

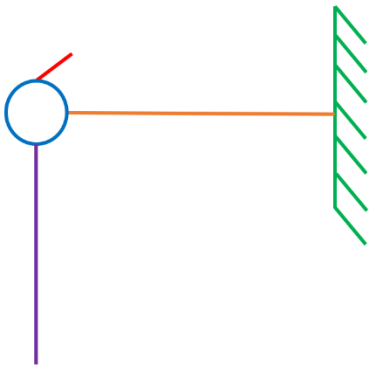

Figure 17: Kinematic diagram of the stand, side view

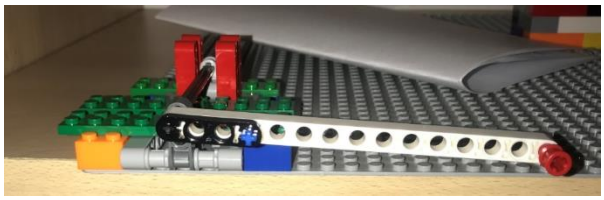

Figure 18: Lego stand used for torsional stiffness, front view

The formula used for each step was the following: $k = \frac{T+Tl}{\theta} = \frac{g*l*m+Tl}{\theta}$

Where,

- T is the torque (N)
- Tl is the torque generated by the lever (N) (see in Annexe 3)
- θ is the angle (rad)
- L is the length of the lever (m)
- m is the mass of the weight applied (kg)
- k is the torsional stiffness (Nm/rad)

Table 2: Torsional stiffness experimental results

$m\ [kg]$	$\theta\ [°]$	$k\ [Nm/rad]$
0.32	57	0.3539
0.47	67	0.4411
0.62	73	0.5334
0.77	74	0.6530
0.87	78	0.6997
0.92	78	0.7398
1.07	80	0.8386

By taking the average of the torsional stiffness values, one can obtain

$$\boldsymbol{k = 0.6085\ Nm/rad}$$

4.1.2. Analytical

This section is dedicated to the calculation of analytical results. Table 3 represents the properties of Lego pieces used for the model.

Table 3: Material properties of Lego material

Properties	E (GPa)	G (MPa)	ρ (kg/m^3)
Lego material	2.588	875	1030 - 1070

The analytical approach is used to calculate the torsional stiffness of a Lego shaft. The goal is to determine an equivalent model of the actual shaft with which one would find similar stiffnesses. For this purpose, three cross sections were analysed; circular, rectangular and mixed.

The formula used to calculate the stiffness is the following:

$$k = \frac{G * J_z}{L}$$

Where,

- G is the shear modulus (Pa)
- J_z is the polar moment of Inertia (m^4)
- L is the length of the element (m) = 95.2mm

The workings in the part of the analysis can be found in the Matlab code annex. And the calculation can be found in Annexe 4.

Circular version

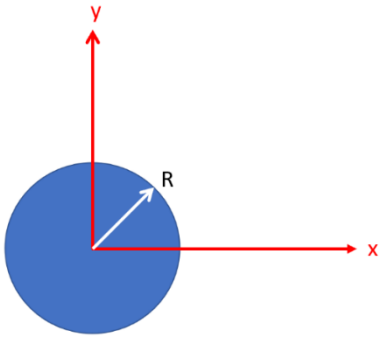

D = 4.72 mm

R= D/2

$$J_z = I_x + I_y$$

$$J_z = 4.8726 * 10^{-11}\ m^4$$

Therefore $\boldsymbol{k = 0.4479\ N/m}$,

Rectangular version

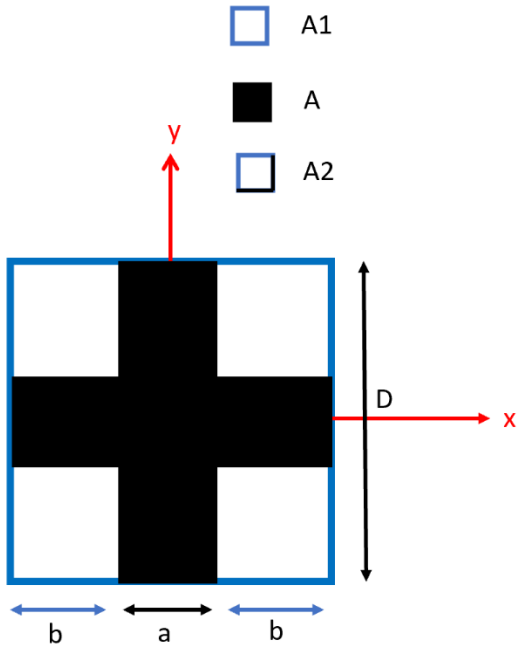

A =A1- 4*A2

a = 1.83mm

b = 1.445mm

A1 = 22.28m^2

A2 = 2.088m^2

D = 4.72mm

R = D/2

$$J_z = I_x + I_y$$

$$J_z = 7.1095 * 10^{-11}\ m^4$$

Therefore; $\boldsymbol{k = 0.6534\ N/m}$

Mixed version: the corners of the cross section are cut by the diameter

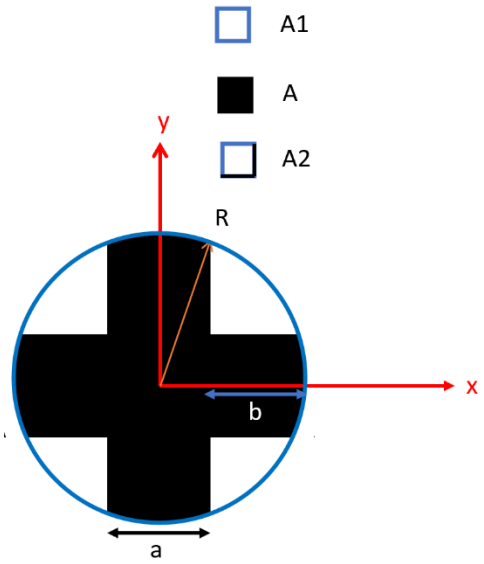

A =A1- 4*A2

a = 1.83mm

b = 1.445mm

A1 = 22.28m^2

A2 = 2.088m^2

D = 4.72mm

R = D/2

$$J_z = I_x + I_y$$

$$J_z = 4.7015 * 10^{-11}\ m^4$$

Therefore; $\boldsymbol{k = 0.4321\ N/m}$

The percentage error between the experimental and the analytical values would give an indication of the accuracy and validity of the models. All percentage errors were done by considering the experimental value as what the analytical value should be, the equation of this being:

$$\%_{error} = \frac{x_{exp} - x_{ana}}{x_{exp}} \times 100\%$$

Where x represents any experimental or analytical value.

Table 4: Percentage error between analytical and experimental results

Model	$\%_{error}$
Circular	26.4 %
Rectangular	-7.4 %
Mixed	29 %

The rectangular model of the cross-section of the shaft was therefore chosen for the following analysis of power losses as it resulted into a slightly higher value than the experimental one.

4.1.3. Assumptions and Sources of Error

The discrepancies between experimental and theoretical results can be explained by the number of assumptions that were made. The main source of error occurs when calculating the torsional stiffness experimentally, the elasticity of the Lego material was not taken into account even though the shaft, the stand and the lever were all made of Lego material. Also, it was noticeable that due to the mass applied, the shaft being tested started to bend. Moreover, the angle between the lever and the horizontal axis was calculated using a protractor which as can be seen in Figure 19 did not allow for best accuracy.

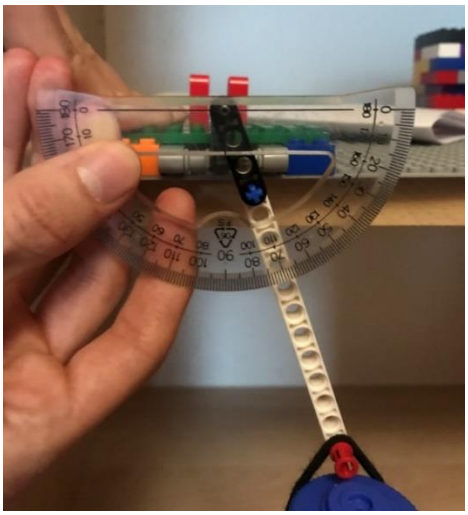

Figure 19: Angle measured using a protractor

Additionally, the mass was measured using a weight scale called QC. PASS which has a precision of 200 grams maximum therefore, since the mass needed was larger than 200 grams, consequently approximations had to be made when pouring the water into its container.

4.2. Power Losses

Any machine that is in motion loses power due to friction, more specifically in this case, any mechanical transmission system that utilizes gears will encounter some losses from input to output. This section of the report aims to illustrate this by presenting an experiment and an analytical model to show this physical phenomenon.

4.2.1. Definition

Power is defined as a scalar quantity of force that is transferred from one distance to another over a certain time. It could also be interpreted as how much torque occurs over a period of rotation, as is the case when considering the mechanical power of an electrical motor. It can be calculated by the following formula:

$$P = T \cdot \omega \ [W]$$

Where T $[Nm]$ represents the torque and ω $[\frac{rad}{s}]$ the rotational speed.

Power loss can be defined as the inefficiency of a mechanical transmission to transmit its input power to its output. This can happen due to friction or by external factors that hampers the machine. For the Lego model, power loss occurs on the LEGO EV3 Medium Motor that runs

the system. Where, ideally the Electric DC Motor would have 100 % electrical efficiency in converting its electric power to mechanical; this does not occur as just like in mechanical transmissions there are losses, due to friction and to electrically related constraints [9].

This report focuses more on the mechanical aspects of the motor, thus the calculations or considerations of this electrical inefficiency is omitted. Another point of interest is to model the losses that occur during the different configurations of the model to better understand the key parameters that affect them. The mechanical power that is produced by the rotational speed of the LEGO EV3 Medium Motor will be referred to as the Input Power of the Lego model. The mechanical power produced by the motor when it is connected to the Lego model under a certain configuration will be known as the Power of Configuration. Therefore, power loss is defined as the difference between the two different powers as this represents the load the rig has on the motor. It can be calculated by the following formula:

$$PL = P_{in} - P_C \ [W]$$

Where P_{in} is the Input Power and P_C the Power of Configuration.

It was defined that there are two main power losses at play when the Lego model is in motion. First, due to the friction between the meshed gear teeth known as Friction Power Loss. Second, due to the torque that is induced unto the system by the different angles of the clutch known as System Power Losses.

4.2.2. Experiment

To obtain experimental data, a method of obtaining reliable and consistent values for the mechanical power had to be determined. The best solution found was to use the data logging capabilities of the LEGO EV3 Intelligent Brick computer, the EV3 software for data acquisition and MATLAB for data processing.

4.2.2.1. Description

The rotational speed with respect to time of the LEGO EV3 Medium Motor that runs the Lego model could be saved as a .csv file by using a EV3 software program. Then, through MATLAB this data could be processed such that the mechanical power of the motor could be calculated. Lastly, with this data the formula for power losses could be used to determine the experimental values for Friction Power Loss and the System Power Losses.

4.2.2.2. Apparatus

Figure 20: Lego EV3 Hardware

LEGO EV3 Intelligent Brick

This hardware (shown on the left of Figure 20) allows for the control of the many accessories of the MINDSTORM set such as the LEGO EV3 Medium Motor. Additionally, it allows for the data logging of the rotational speed of the motor with respect to time.

LEGO EV3 Medium Motor

This hardware (shown on the right of Figure 20) is an electric DC motor that uses the 10 V DC power supply from the Intelligent Brick to run. Depending on the command, the motor can run in a clockwise or counter clockwise direction. Through the EV3 software program, the power percentage of the motor can be determined; as such, for this experiment the power percentage of the motor was 100%. Any lower percentage proved to be detrimental to the experiment because the excess power was used to power a controller in the hardware such that a constant rotational speed could be achieved. This hampered our results as we were interested in studying how the mechanical power decreases throughout the different configuration of the Lego model and not how effective the controller is.

To obtain the specifications of the motor, the values obtained from Philohome's LEGO® 9V Technic Motors compared characteristics [10] were used. This website provided experimental data of the capabilities of the many LEGO motors and as such provided the following information for the motor used in the model:

Table 5: Specifications of LEGO EV3 Medium Motor

Estimated Power supply	Torque	Stalling Torque
9 V – 12 V	6.64 Ncm	15 Ncm

With this, the capabilities and limits of the motor were known. The experimental data obtained from the experiment was compared with the results of the website and thus were corroborated.

EV3 Software Program

This software allows for the creation of a program to log data of the rotational speed of the motor with respect to time. This data can be saved in different kinds of formats, for this project it was chosen to be saved as a .csv file (comma separated value file) for ease of use in MATLAB. After much trial and error, a minute showed us the best representation of how the motor functions. A lower period of time provided information that did not converge to a certain value, on the other hand a higher period of time provided too much unnecessary data that already converged to a final value. This program was created by using the symbolic representation of computational functions of the software. Figure 21 represents this symbolic representation in the EV3 software, while Figure 22 is the flow diagram of the logic behind the program.

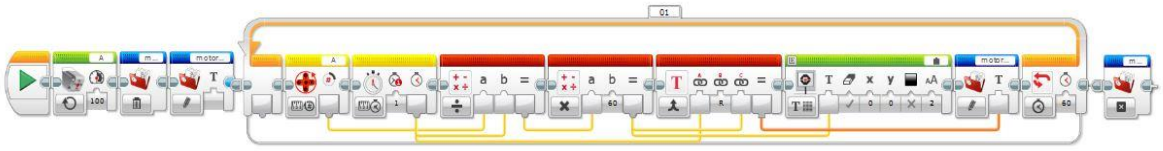

Figure 21: EV3 Software Program for RPM Data Logging

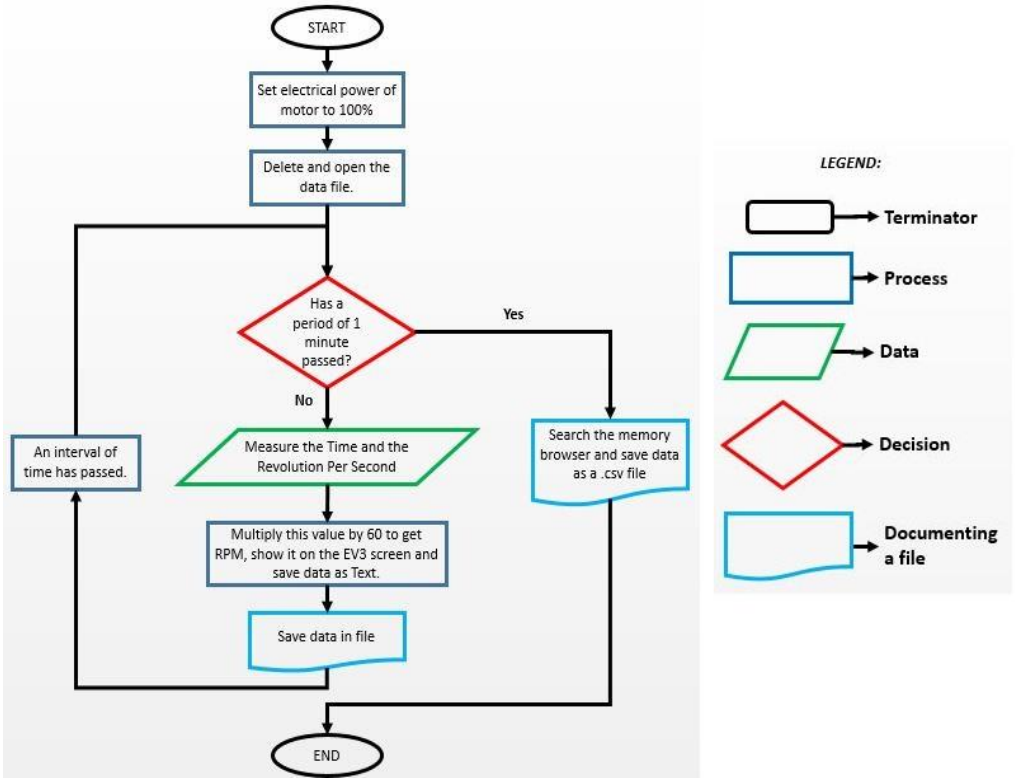

Figure 22: EV3 Software Program Flow Diagram

The rotational speed acquired throughout a period of 60 seconds is then imported to MATLAB for further data processing. As already stated, the mechanical power of an electric motor is the multiplication of its torque and rotational speed. Thus, whatever the rotational speed is at a certain time is multiplied by the constant torque of the motor of 6.64 Ncm.

4.2.2.3. Procedures

To acquire the experimental data for the power losses, the following steps were followed:

1. Connect the LEGO EV3 Medium Motor to the Intelligent Brick and this to a computer via a USB cable.
2. Open the EV3 Software Program.
3. Place the motor in the designated position for the Only Motor test.
4. Run the Program to make the motor run for 60 seconds, make sure to not cause any disturbances or vibrations on the table the Lego model is on, to ensure accuracy. Save the RPM data from the memory browser with the following name: motor100-A-OM.csv. Make sure to save it in the designated LegoEV3_Data folder next to the MATLAB Analysis.m code.

5. Connect the motor to the Lego model, make sure there is no induced torque unto the system by checking the torsion in the Torsional Demonstration Shaft. Repeat step 4 and name the file: motor100-B-0T.csv.
6. Disconnect the motor from the Lego model and apply an induced torque by twisting the clutch by 45 degrees.
7. Connect the motor to the Lego model with induced torque and run the program, repeat step 4 and name the file: motor100-C-45T.csv.
8. Repeat steps 6 and 7 until you have information of the RPM of the motor for the intervals of 45, 90, 135 and 180 degrees of rotation of clutch. Follow the same naming criteria, where after motor100 each successive file has the next letter of the alphabet and designate the degrees of torque with .csv at the end.

4.2.2.4. Sources of Error

The possible sources of error that could be found during the experiment were the following:

- By experimenting with the motor, the exact same RPM could not be reproduced for the same configuration; there were always small deviations. Only a full set of tests (running with only the motor, connecting it to the model and running it with induced torque) could be compared with each other and used to calculate the power losses.
- As Lego pieces were used, the material they are made up of has a plastic behaviour from which deformations are easily created. Thus, as more experiments were done the Lego components, mainly the shafts, eroded ever so slightly such as to decrease the consistency of the experimental results. Nonetheless, this changes in shape are small and thus neglected in the final calculations but still are talked about as they could prove to be a source of error.

4.2.3. Analytical Model

The purpose of obtaining experimental data was to corroborate a hypothesis, that being that the physical dimensions of the Lego model are key parameters in the power losses at play. To validate the analytical models, the percentage error between the experimental and the analytical values was calculated. This equation is the same one used in the Torsional Stiffness section 4.1.

4.2.3.1. Friction Power Loss

Any surface that slides with another will produce friction, this phenomenon is universal and occurs between the surfaces of the meshed gear teeth of the Lego model when it is run. It is important to understand where this concept comes from but more so to quantify it. The hypothesis used for this calculation stems from the investigative report on friction coefficient of FZG lubricated gears [11].

In an industrial gear box, there exists power dissipation and thus heat evacuation. Inside the box there are mechanical components that induce a resistance to the motion of the gears that produce a power loss. Through an energetic balance, the power lost by the many components inside, such as the lubricant, bearings, and seals, will be transformed into heat. This heat will then be evacuated through the known means of heat transfer: conduction, convection, and radiation. This report will not focus on the heat transfer aspect of the gearbox as the temperature

differences produced by the Lego model are too small to measure and thus the mathematical model could not be validated with experimental data.

The report aimed to illustrate an analytical and experimental model on the power losses at play of the FZG test rig. They concluded on equating the power losses to the heat evacuated from the system, by placing temperature sensors in the gearbox they acquired experimental data to validate their research. This report will only utilize their power losses equation and redefine it such that it fits the current Lego model. As many of the components that make up a traditional gearbox are missing on the Lego model, most of the equation is equal to 0. To help illustrate this concept, the following Figure 23 shows on the left the original schematic view of the FZG gearbox's power loss and heat evacuation and on the right the equivalent representation on the Lego model test gearbox.

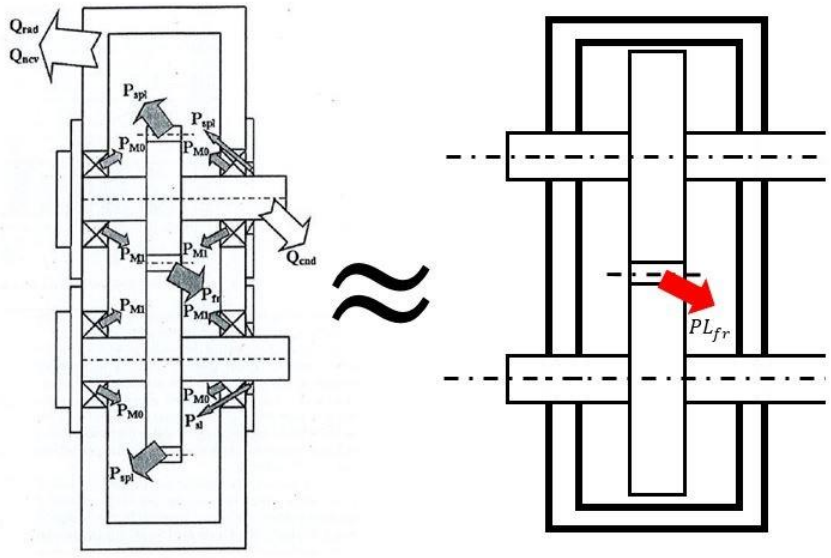

Figure 23: Schematic view of FZG gearbox and Lego model gearbox

The equation for power losses and heat dissipation in a conventional FZG gearbox is the following:

$$P_L = Q_{Tot} \rightarrow P_{fr} + P_{M1} + P_{spl} + P_{M0} + P_{sl} = Q_{rad} + Q_{cnv} + Q_{cn}$$

Where P_{fr} is the power loss due to friction between meshed gear teeth, P_{M1} the rolling bearing friction loss, P_{spl} the gear churning losses, P_{M0} the bearing churning losses, P_{sl} the seal losses, and the subsequent Q's the heat transfer mediums. Due to the simplicity of the Lego model, most of these variables can be equated to 0 as there is no lubricant to cause churning, no bearings to cause rolling friction and no seals as there is no lubricant. The heat dissipated by the Lego model can be ignored as the temperature difference is negligible when under operation. The only power loss at play is the friction between meshed gear teeth according to the mathematical model proposed by the investigative report.

Therefore, the Friction Power Losses is defined by the following equation:

$$PL_{fr} = \pi \cdot \left(\frac{1}{z_1} + \frac{1}{z_2}\right) \cdot \left(1 - \left(\frac{g_f + g_a}{p_b}\right) + \left(\frac{g_f}{p_b}\right)^2 + \left(\frac{g_a}{p_b}\right)^2\right) \cdot P_{in} \cdot \mu_m \; [W]$$

Where the subscript 1 refers to the driving gear (pinion), and subscript 2 to the driven one.

The variable $z_{1,2}$ are the number of teeth of its respective gear, g_f is the length of approach path, g_a is the length of recess path, p_b is the base pitch of the gears. The equations for these gear parameters are in the annexe 5 and are based off the working found in reference [12]. P_{in} is the input power of the system already defined in a previous section 4.2.1. and μ_m the mean friction coefficient.

As the only material to consider for the friction between meshed gear teeth of the model is what the Lego gears are made of, the mean friction coefficient was assumed to be the one of Acrylonitrile Butadiene Styrene plastic: $\mu_m = [0.11 - 0.46]$. This range of values was obtained from Typical Properties of Generic ABS [13] which were obtained from the ASTM D1894 test method for friction coefficient calculation.

4.2.3.2. System Power Loss

All the mathematical workings for the following equations are in annexe 5.

A torque acting in the opposite direction of motion to an electric motor will cause it to run at a lower rpm. This is because the induced torque must first be overcome and then exceeded such that rotation occurs. In the case of the Lego model and the real FZG test rig, it is of interest to study how the gears would react to such kinds of torque. In both contraptions, the ultimate goal of the clutch is to induce torsion into the system. It would then be of great interest to quantify this amount as function of rotation of the clutch as the input, and the torque as the output. After which, this induced torque can be used to calculate the power losses.

After studying the Lego model extensively, an equation for the induced torque unto the system from the rotation of the clutch was formulated. This formulation was done by equating the many physical phenomena at play on the Lego model to each other; as in a mathematical causal relation between the many components was determined. The overall equation for this induced torque was determined to be the following:

$$T_S = k_{eq} \cdot \phi_c \; [Nm]$$

Where k_{eq} is the equivalent torsional stiffness calculated of the entire model and ϕ_c the apparent angle of twist produced by the rotation of the clutch.

The calculation of the System Power Loss would be the following:

$$PL_s = P_{in} - (T - T_{fr} - T_s) \cdot \omega_{in}$$

Where P_{in} is the input power of the motor, T is the constant torque of the LEGO EV3 Medium Motor, T_{fr} the estimated torque produced by the Friction Power Loss, T_s the induced torque unto the system from the clutch and ω_{in} the input rotational speed of the motor. The following is the equation for T_{fr}: $T_{fr} = \frac{PL_{fr}}{\omega_{in}}$

To obtain the equation for k_{eq} a torsional analysis of the test rig by considering it as a single shaft was done. To obtain the equation for ϕ_c an angle of twis, an analysis was done on each shaft of the Lego model.

Torsional Analysis

One could think of the Lego model when it is under a locked configuration as a simple machine. Where the rotation of the clutch results in a certain amount of torque to be induced unto the system once the clutch is linked back together and the model is now in an unlocked configuration (free to rotate). Subsequently the relation between this input and output is determined by the torsional stiffness of each of the components of the model.

To help illustrate this, the following Figure 24 shows a Free Body Diagram of the Locked configuration on the left and its equivalent single shaft on the right; where spring and inductor symbols were used to help illustrate the relation between two points. The spring symbol represents torsional stiffness and the inductor symbol either a gear or torque ratio.

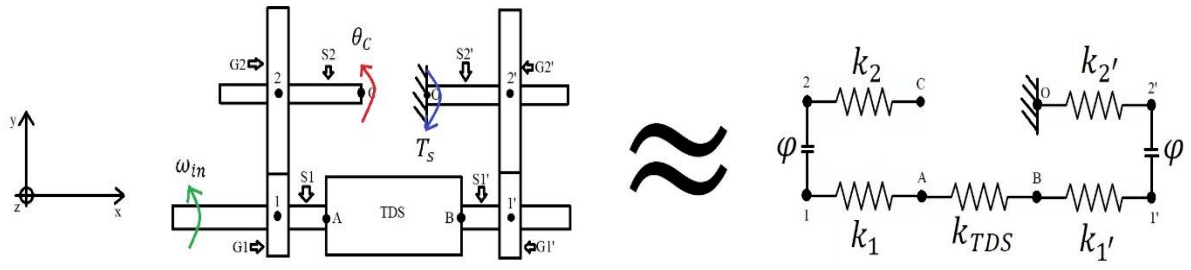

Figure 24: FBD of Torsional Analysis of Locked Configuration of the Lego Model

After analysing this FBD, the following equation was deduced for the equivalent torsional stiffness:

$$k_{eq} = \left(\frac{3JG}{3L_{2'} + 3\varphi L_{1'} + \varphi L_{TDS} + 3\varphi L_1 + 3L_2}\right)\left[\frac{Nm}{rad}\right]$$

The Polar Moment of Inertia J used by this equation is the analytical results of the torsional stiffness study of the Lego Shaft. The variable G is the shear modulus of the Lego material. All Ls represent the effective length for torsion of each shaft it refers to by its subscript, this is the actual length of the shaft that is twisted; mathematically it is the length between one point to another, for example: $\overrightarrow{C2} = -L_2 \cdot \hat{x}$. These are the measured effective lengths for torsion of the Lego model:

Table 6: Effective Lengths for Torsion of the Lego Model

L_1	L_2	L_{TDS}	$L_{1'}$	$L_{2'}$
43 mm	48 mm	130 mm	98 mm	122 mm

The variable φ is the gear ratio: $\varphi = \frac{\theta_2}{\theta_1} = \frac{Z_1}{Z_2}$

Where as $\frac{1}{\varphi}$ is the torque ratio: $T_1\theta_1 = T_2\theta_2 \rightarrow \frac{T_2}{T_1} = \frac{\theta_1}{\theta_2} = \frac{1}{\varphi} = \frac{Z_2}{Z_1}$

Where z is the number of teeth, the subscript 1 refers to the driving gear and the subscript 2 to the driven gear.

Apparent Angle of Twist Analysis

To obtain the apparent angle of twist, a Free Body Diagram (shown in Figure 25) focusing on the torques produced by rotating the clutch was made.

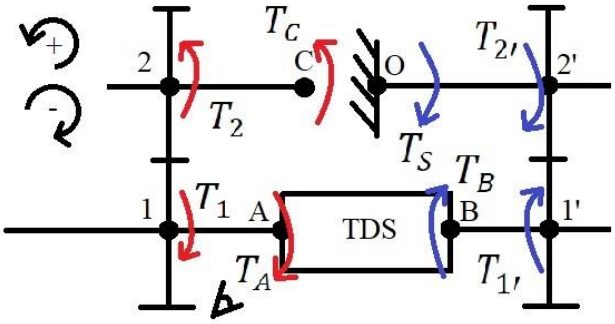

Figure 25: FBD of Angle of Twist Analysis of Locked Configuration of the Lego Model

The torque created by rotating the clutch by a certain degree is represented by red arrows, and the reaction torque produced by the grounded section of the Lego model by the blue arrows. Essentially, half the model twists in one direction while the other in the opposite; this ultimately leads to a torsion unto the system, which after the clutch is placed back into an unlocked configuration will sustain this torsion. Thus, the torque at the grounded section of the Lego model is the one used in the System Power Losses equation T_s. A key area that helped to determine the equation for the apparent angle of twist was the Torsional Demonstration Shaft (TDS). This shaft was placed under torsion from two different sides, the rotation of the clutch and the reaction torque to this rotation from the grounded point. This is illustrated in the following figure:

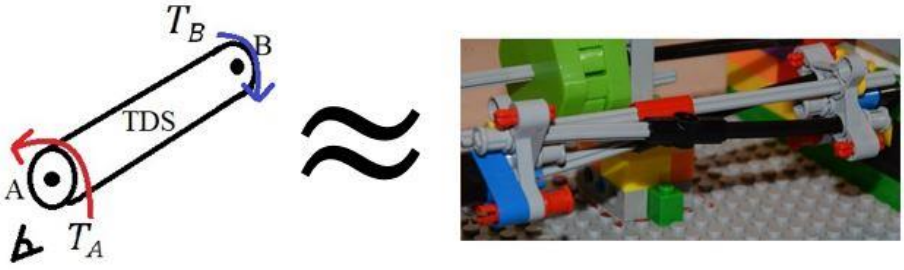

Figure 26: Torsion imposed on the Torsional Demonstration Shaft

By analysing the FBD and the TDS, the following equation was deduced for the apparent angle of twist:

$$\phi_c = \frac{L_{2'}(L_{TDS} - 3L_1)}{(3L_{1'} + L_{TDS})L_2}\theta_C \ [°]$$

Where the Ls are the effective lengths for torsion from the previous section, and θ_C the angle of rotation the clutch undergoes. Lastly, by substituting in the equivalent torsional stiffness of the Lego model and the apparent angle of twist into the T_s one obtains a final equation of:

$$T_s = \left(\frac{3JG}{3L_{2'} + 3\varphi L_{1'} + \varphi L_{TDS} + 3\varphi L_1 + 3L_2}\right)\frac{L_{2'}(L_{TDS} - 3L_1)}{(3L_{1'} + L_{TDS})L_2}\theta_C \ [Nm]$$

Sources of Error

This previous equation has assumptions which could prove to be sources of error such as:

- The measured effective lengths for torsion were considered to be the length of the shaft that is under torsion. These measurements are prone to human error.
- The overall analytical power losses is cumulative, thus all errors of previous sections are still affecting the results of the next section. As in the analytical value for the Friction Power Loss has a direct effect the System Power Loss.
- The shape of the Torsional Demonstration Shaft influences the overall equation. Thus, any errors produced by the assumptions of its shape are magnified.

4.2.4. Results

The following are the results for the power losses calculations of the experiments done with the Lego model and the analytical model using the MATLAB code called Analysis.m used for data processing. A flow diagram describing the logic of the code is in annexe 6. The following igure is the mechanical rotational speed produced by the motor throughout 60 seconds for 6 different configurations:

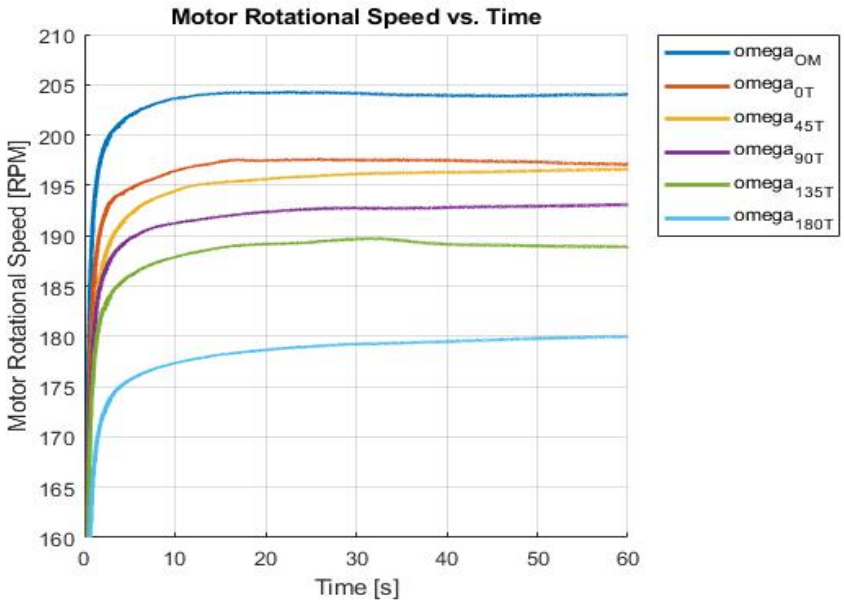

Figure 27: Motor Rotational Power vs. Time

From this data, the experimental and analytical models are applied. This results in the following figure, where the Friction Power Loss plot is placed on the left and on the right the System Power Losses one:

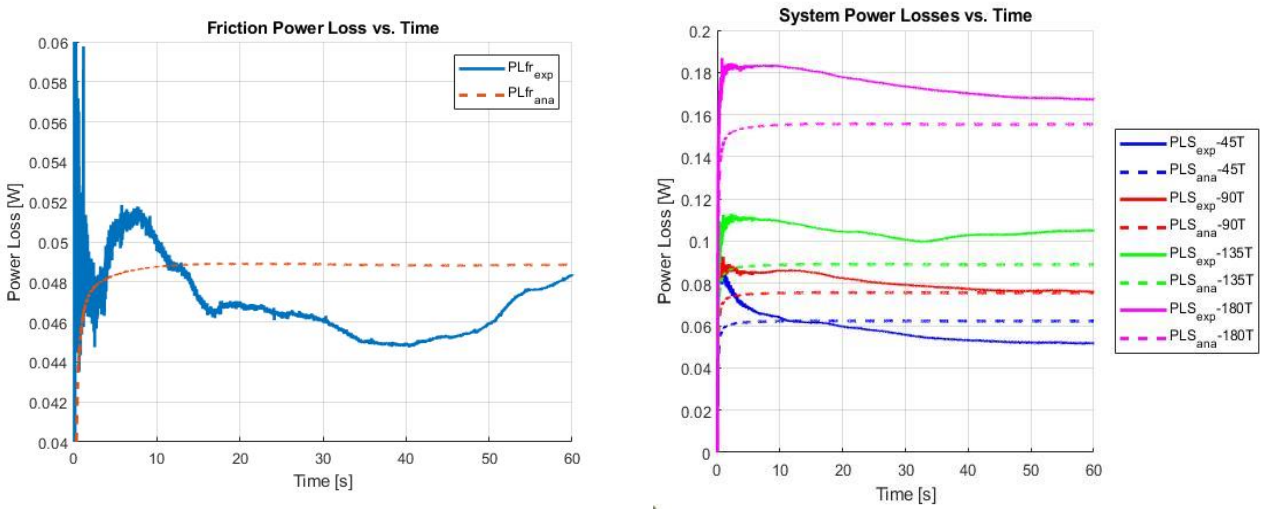

Figure 28: Power Losses vs. Time

To acquire a mathematical validity to the analytical model with respect to the experimental one, the subsequent tables of values were produced. As more and more torsion was induced unto the system through the clutch, the effective length of torsion of a shaft changed. More precisely, only the length of the Torsional Demonstration Shaft had increased. After placing the Lego model in a certain configuration, new measurements were taken of all the shafts. After all the experiments were completed and the shafts, measured, it was concluded that only L_{TDS} changed ever so slightly. The values of this length throughout each configuration are noted in the Table 7 below:

Table 7: Change of Length of TDS through the different configurations

θ_c [°]	45	90	135	180
L_{TDS} [mm]	130	130	130	131

Table 8: Measure induced torque unto system by clutch

θ_c [°]	T_{s_exp} $[Nmm]$	T_{s_ana} $[Nmm]$
45	0.523	0.627
90	1.572	1.253
135	2.706	1.879
180	5.975	4.989

Where θ_c are the degrees of rotation of clutch and L_{TDS} is the length of the Torsional Demonstration Shaft, and T_{s_exp} are the experimental values of induced torque and T_{s_ana} the analytical values of induced torque.

Table 9: Results of Friction Power Losses

$\overline{PL}_{fr\_exp}$ $[W]$	$\overline{PL}_{fr\_ana}$ $[W]$	$\%_{error}$ [%]
0.047	0.049	-3.66

Where $\overline{PL}_{fr\_exp}$ is the experimental mean value for Friction Power Loss, $\overline{PL}_{fr\_ana}$ is the analytical mean value for Friction Power Loss, and $\%_{error}$ the percentage error.

Table 10: Results of System Power Losses

θ_c [°]	$\overline{PL}_{S\_exp}$ $[W]$	$\overline{PL}_{S_{ana}}$ $[W]$	$\%_{error}$ [%]
45	0.058	0.062	-6.56
90	0.080	0.075	+6.42
135	0.105	0.089	+15.26
180	0.174	0.155	+11.12

Where θ_c are the degrees of rotation of clutch, $\overline{PL}_{S\_exp}$ are the experimental mean values for System Power Loss, $\overline{PL}_{S_{ana}}$ are the analytical mean values for System Power Loss and $\%_{error}$ are the percentage errors. The overall mean percentage error, accounting for both Friction and System Power Losses, is of **+4.52 %.**

4.3. Validation Experiment

4.3.1. Description

To ensure that the analytical power losses model is accurate, a validation experiment was proposed which aimed to simulate the amount of torque when the clutch is loaded at different degrees. To perform this, a string is attached on the shaft where the clutch is and at the end of the string a water bottle with a certain amount of water is attached. Since the radius of the shaft d is known (2.36 mm), one can calculate the amount of torque the weight of the water bottle imposes on the shaft. This is used to validate the analytical model and confirm the amount of torque the clutch mechanism creates when rotated in different positions.

In practice, sewing thread was used and attached to the shaft that linked the right clutch pad to the slave box. This was done arbitrarily and any of the other shafts could have been used. The string was attached to a plastic bottle which hanged above the ground. A limit of only 10 seconds of tests was imposed by the height of the tables on which the Lego model was placed, ideally a higher height would have allowed for more test time however there was no structure that allowed this. The experiment was performed by imposing the largest amount of torque and then decreasing it onwards. This translates to removing a certain amount of water each time by using a scale. Finally, the data was recorded using the LEGO EV3 Medium Motor and the EV3 Intelligent Brick. From the following

Figure 29: Validation experiment set up

relation, the mass of water needed to simulate the same amount of torque as that of the clutch in different positions can be determined by the following equation:

$$T = W * d = m * g * d \rightarrow m = \frac{T}{d * g}$$

Figure 30: Diagram of the validation experiment

4.3.2. Results

The following table shows the values for the results of this experiment.

Table 11: Results of measured torque for validation experiment

θ_c [°] angle of torque	T_{s_ana} [Nmm]	m [g]	T_{exp} [Nmm]
0	0	0	0
45	0.626	27	1.52
90	1.253	54	1.869
135	1.874	81	2.455
180	2.506	108	4.090

Where θ_c are the degrees of rotation of clutch, T_{s_ana} the analytical value for the induced torque unto the system, m the mass of the hanging weight and T_{exp} the experimental value for the induced torque unto the system.

The following two figures represent the results of the experimental for power losses when the Lego model was submitted to the validation experiment. Figure 31 is the plot of the motor mechanical power with respect to time, on the left of Figure 32 a plot of the friction power loss with respect to time is placed and on the right of Figure 32 a plot of the system power loss with respect to time:

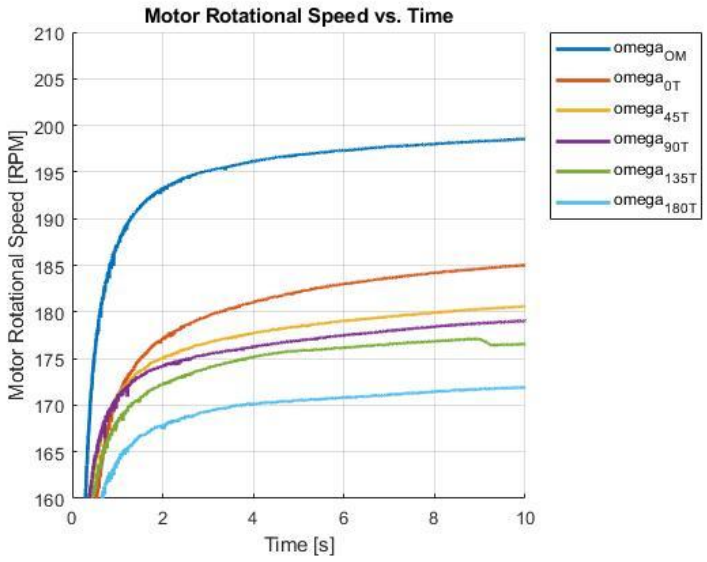

Figure 31: Motor Rotational Speed vs. Time of Validation Experiment

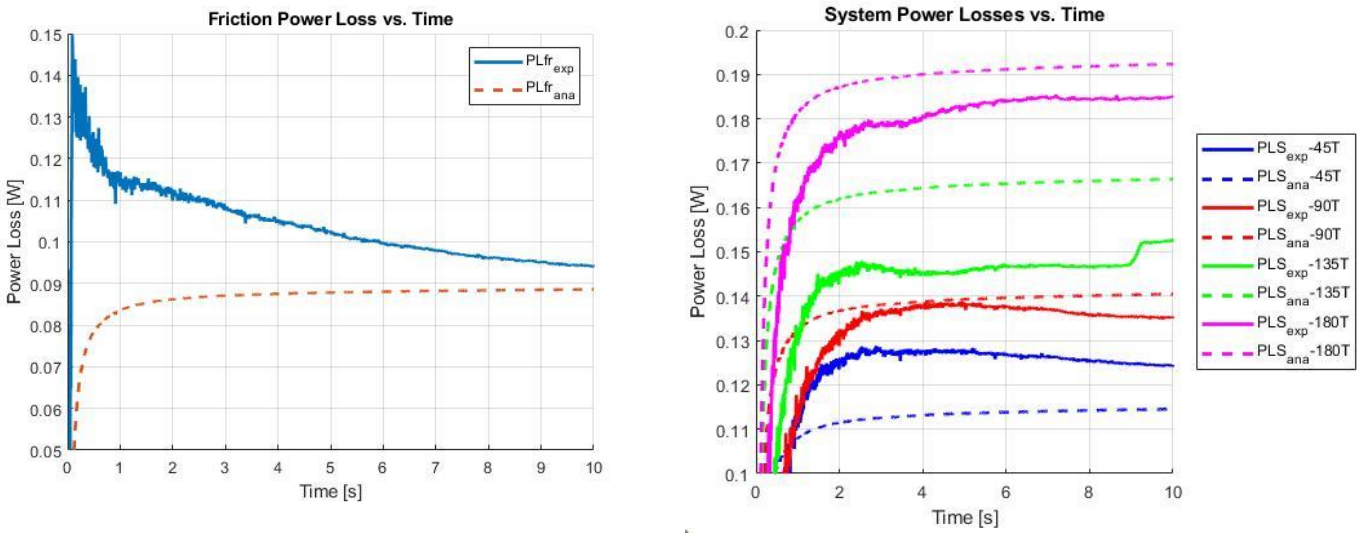

Figure 32: Power Losses vs. Time of Validation Experiment

From the calculations done by the Analysis.m file, the following tables have the values of interest obtained:

Table 12: Results of Friction Power Losses from Validation Experiment

$\overline{PL}_{fr\_exp}$ $[W]$	$\overline{PL}_{fr\_ana}$ $[W]$	$\%_{error}$ [%]
0.089	0.089	-0.993

Where $\overline{PL}_{fr\_exp}$ is the experimental mean value for Friction Power Loss, $\overline{PL}_{fr\_ana}$ is the analytical mean value for Friction Power Loss, and $\%_{error}$ the percentage errors.

Table 13: Results of System Power Losses from Validation Experiment

θ_c [°]	$\overline{PL}_{S\_exp}$ $[W]$	$\overline{PL}_{S\_ana}$ $[W]$	$\%_{error}$ [%]
45	0.121	0.115	+4.65
90	0.128	0.141	-10.28
135	0.140	0.167	-19.22
180	0.174	0.193	-10.81

Where θ_c are the degrees of rotation of clutch, $\overline{PL}_{S\_exp}$ are the experimental mean values for System Power Loss, $\overline{PL}_{S\_ana}$ are the analytical mean values for System Power Loss and $\%_{error}$ is the percentage error.

Even though, the measured torques differ far greater in this experiment than those of the conventional experiment, the overall mean percentage error of the analytical power loss compared to the experimental is of **-7.33 %.** Where in the previous results, the length of the Torsional Demonstration Shaft changed on the last interval of torque, here this length was determined to be a constant: $L_{TDS} = 131\ mm$ for all intervals of rotation.

This percentage error remains in a good margin of error as there are many factors that could have affected the results. For example, since the water bottle swinged as it was pulled up, the string came into contact momentarily with the hole in the plate which could easily affect the torque. Furthermore, when measuring out the amount of water required, the quantities were not exact which led to the development of additional errors.

5. Discussion

The percentage error between the analytical and experimental models for the power losses is of 4.52 % for the conventional experiment and of -7.33 % for the validation experiment. These low percentage errors, validates to an extent the mathematical workings done on the Lego model. The equations used were based on many assumptions, and to simplify the analytics, the Torsional Demonstration Shaft (TDS) shape for its Second Moment of Inertia played a major role. Thus, any assumptions made on this shape had repercussions on all the working.

Ultimately, the induced torque unto the system by the rotation of the clutch had two varying components: that being the rotation of the clutch and the length of the TDS. After much trial and error, it was determined that as more torque was introduced, the TDS would slowly try to expand as the contraction of the 3 shafts would create a tension force pushing the components further apart. This realization is what allows the analytical model to be as accurate as it is. Nonetheless, more experiments would have to be done with a more reliable motor such as to validate this hypothesis.

Furthermore, it is important to note that the torque chosen for the motor was considered constant for each test that was carried out. However, when recording data with the EV3 Data Brick, it was noticeable that the more torque induced into the system, the more the batteries of the brick would get less effective and therefore might not transmit enough electrical energy for the motor to run a constant torque. This is a hypothesis but may have been a better idea to consider the power of the motor as a constant torque.

6. Future Developments

It was decided to focus the main part of this project on the analysis of Power Losses, however many side projects were carried, some of which were not successful or would have requested more time.

6.1. 3D printed gears

Aforementioned, the two pair of gears chosen for the final Lego Model were made of four identical wheels due to not enough choice of Lego gears. Therefore, Solid-Edge model of a couple of wheel and pinion was created using Gear designer so that it would be as similar as possible to the actual gear by having the same module and ratio, when keeping the same centre distance and face width as the yellow Lego gears so that it fits into the Lego model. The models were created to possibly 3D-printed them.

In Figure 33, the CAD model of gear is presented:

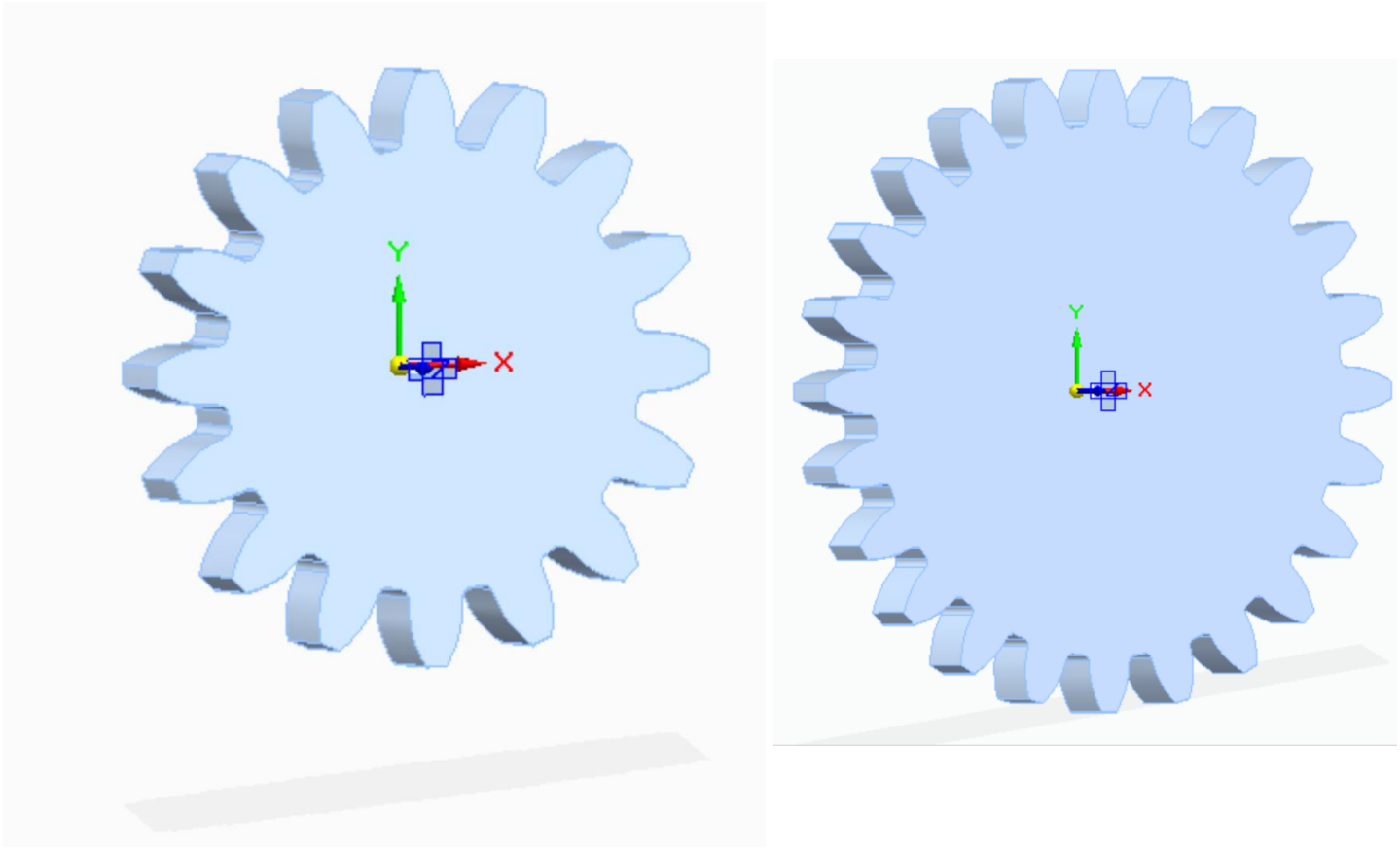

Figure 33: CAD model of the gears

6.2. Friction induced vibrations.

One of the aspects of the project was turned towards understanding the power losses of the FZG test rig from a vibrations point of view. The idea was to establish a correlation between the vibrations that are recorded using sound, and the power losses linked to those vibrations. [14]. An increased torque in the system is expected to produce more noise due to the larger

amounts of forces the gears experience. This causes more friction between the gears and therefore generates more vibrations. The objective was then to be able to isolate the friction induced vibrations and to quantify the amount of power losses found when using the recorded sounds and compare it to the analytical model.

To perform this experiment, a microphone was placed at a close distance to the meshing point between the gears. The test rig was run without any induced torque in the system for a period of 60 seconds. This was done to obtain a reference for the profile of the sound that can then be compared to the other sounds. This experiment was performed again with different amounts of torque in the system. In total three tests were performed with no torque, torque when clutch is rotated 90° and a final one when the clutch is rotated at 180°. By subtracting the noise generated by all the other components in the test rig model (motor, shafts, …) this would allow for visualisation of the noise generated by the gears only.

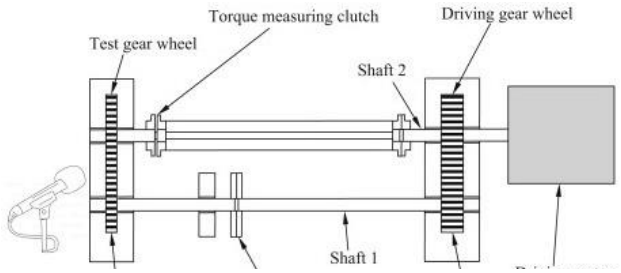

Figure 34: vibrations experiment setup [16]

Once the noises of the experiments were recorded, they were implemented into the Signal Analyser feature of MATLAB. Figure 35 shows the Power spectrum when 0, 90 and 180° f torque is applied into the system:

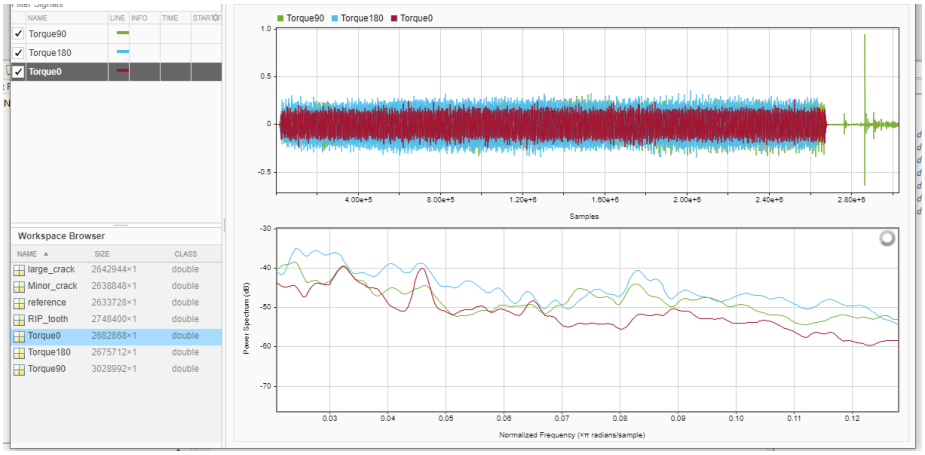

Figure 35: Power spectrum of the recorded sounds

The power spectrum representation computes the power within the signal over its' frequency based on a finite set of data. On one hand, the experiment was successful in demonstrating that a higher amount of torque generates a larger amount of noise which is clear when observing the power spectrum. What can also be observed is that generally, the curves of all three recordings follow similar forms which would suggest a certain regularity in the vibrations that may be easier to analyse. Additional errors contribute to obtaining a false result due to insufficient knowledge about the equipment (sensitivity of the microphone used, distance placed, orientation of the microphone, …) used in the actual models. This is one of the key

aspects where the project could have been expanded upon. However, due to the timeframe set for this project, it was considered preferable to focus on what had already been achieved.

6.3. Tooth crack test

Another path was explored and focused on presenting in broad some of the work performed by real engineers that study vibrational acoustics in mechanical systems which allows them to detect and analyse mechanical phenomena. One of the interests in analysing the vibrations generated by gears is to observe potential cracks or defects such as micro-pitting on the tooths. The objective of this experiment was to simulate a crack by creating a defect on the gear and to record the sounds generated. Three tests were completed, each one with an increasing defect until reaching breaking point which was simulated by removing an entire tooth. What was expected to happen is observe periodically large spikes in the spectrum analysis which would indicate that there is a large defect at that place.

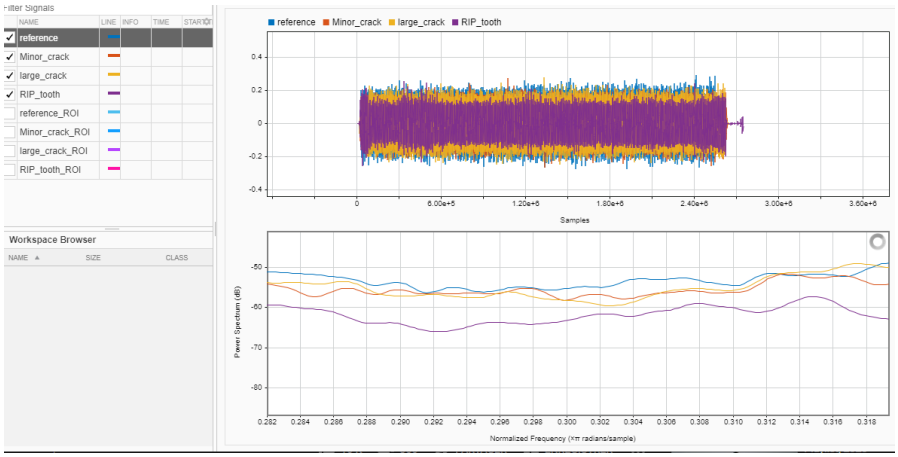

Figure 36: Tooth crack recordings

The graph of all of the tests where there is a defect in one of the gears is always under the reference line which is the one where the gears are in perfect condition. An interesting element that was visible was the last test as power spectrum generated by the gears shows significantly less power generated. This was expected as severe damage to gears like a tooth breaking off significantly reduces the amount of power that is transmitted via the gears. One of the more contradictory findings was that the “large_crack” graph appears to generate more power than the “minor_crack”. As with the “RIP_tooth” graph, it would seem logical that a larger defect would cause more power losses and cause less noise and less power to be generated. Furthermore, the large peaks that were expected to show on the spectrum caused by the effects were not visibly present. The future goals would have been to reduce or get rid of the white noises as well as having a better microphone to work with, for instance a microphone having a better sensitivity.

Conclusion

The objective of understanding the entire mechanism of an FZG test rig as well as representing the overall concept using Legos has been achieved. A final model was proposed with reduced vibrations to use for Power Losses analysis including a 3D printed clutch which allows for more experiments. The effect of the torque on the mechanical loop could be clearly observed thanks to the Torsional Demonstration Shaft.

The process of building this Lego model was performed based on the elements and constraints that were given to us. As of such, it was not possible to build a model to scale nor was it the objective in this case. The focus was brought onto designing a functional model that could be reliable enough to perform experiments on. It was one of the reasons why the large gears were chosen over having a gear ratio.

The purpose for which the analytical model for power losses was made is for designing. The knowledge of knowing which parameters have an effect of the phenomenon at play allows for the specification of the dimensions. In other words, because there are equations that have been proven to create a valid model compared to experimental results, one can follow them to reverse engineer a model of a certain size. To create a Lego model capable of sustaining 10 Nmm of torque to either study power losses or how 3-D printed Lego gears of a certain material would sustain this load, one could do so by specifying the lengths of the test rig according to the equations presented. The equations of Friction Power Loss and the induced torque unto the system by rotation of clutch are a powerful tool. They allow for the dimensioning of a Lego model to fit an operational specification.

This project has the potential to be developed in many ways based on what was already achieved. In future projects, a deeper focus can be brought onto the subjects which did not have the time to be fully explored such as vibrations.

Bibliography

[1] "Wikipedia," [Online]. Available: 1. https://en.wikipedia.org/wiki/Reverse_engineering. [Accessed 04 03 21].

[2] STRAMA-MPS, "Tecnical Journal FZG News," *STRAMA-MPS*, p. 12, Unknown.

[3] K. S. Gears, "Lubrication of Gears," Unknown. [Online]. Available: https://khkgears.net/new/gear_knowledge/gear_technical_reference/lubrication-of-gears.html. [Accessed 12 11 2020].

[4] SKF, "SKF," [Online]. Available: https://recondoil.com/gear-oil-guide/#tab-con-9. [Accessed 17 12 2020].

[5] SKF, "SKF RecondOil," [Online]. Available: https://recondoil.com/gear-oil-guide/#tab-con-9.

[6] P. O. T. T. K. M. Bernd-Robert Hoehn, "TEST METHODS FOR GEAR LUBRICANTS," 2008.

[7] k. lubrication, "FZG four square oil tester," 7 07 2007. [Online]. Available: https://www.youtube.com/watch?v=dxXulu3zrL8. [Accessed 15 12 2020].

[8] J. V. Boris Kržan, "researchgate.et," 22 03 2006. [Online]. Available: https://www.researchgate.net/publication/27192091_TRIBOLOSKA_SVOJSTVA_MAZIVA_IZ_OBNOVLJIVIH_IZVORA. [Accessed 17 12 2020].

[9] "Quora," 2019. [Online]. Available: https://www.quora.com/Why-is-the-efficiency-of-an-electric-motor-less-than-100#:~:text=While%20there%20is%20less%20friction,have%20thanks%20to%20air%20resistance.&text=Electric%20motors%20have%20an%20efficiency,loss%20through%20any%20mechanism%20imaginabl. [Accessed 03 04 2021].

[10] Philohome, 15 May 2020. [Online]. Available: https://www.philohome.com/motors/motorcomp.htm. [Accessed 7 03 2021].

[11] J. S. A. B. C. S. R. L. A. I. R. Martins, "Friction Coefficient in FZG gears lubricated with industrial oils: Biodegradable ester vs. mineral oil," ELSEVIER, Porto, Portugal. Manheim, Germany. Eibar, Spain., 2005.

[12] Mehran University College of Engineering and Technology Khairpur, "slideshare," 12 December 2012. [Online]. Available: slideshare.net/AAhadNoohani/gears-mom2-2. [Accessed 6 February 2021].

[13] UL, "PROSPECTOR," 2020. [Online]. Available: plastics.ulprospector.com/generics/1/c/t/acrylonitrile-butadiene-styrene-abs-properties-processing. [Accessed 4 February 2021].

[14] F. V. P. V. Y. DIAB, *prediction of power losses due to tooth friction in gears*, Toronto, 2004.

[15] "UNSA," [Online]. Available: 2. https://www.usna.edu/EE/ee301/supplements/Rotating%20DC%20Motors%20Supplement%20II.pdf. [Accessed 04 03 2021].

[16] H. Anton Planitz, "Science Direct," June 2009. [Online]. Available: https://www.sciencedirect.com/science/article/abs/pii/S0301679X09000073. [Accessed 15 03 2021].

Annexes

Annexe 1 : Picture of the key and the slot for the key

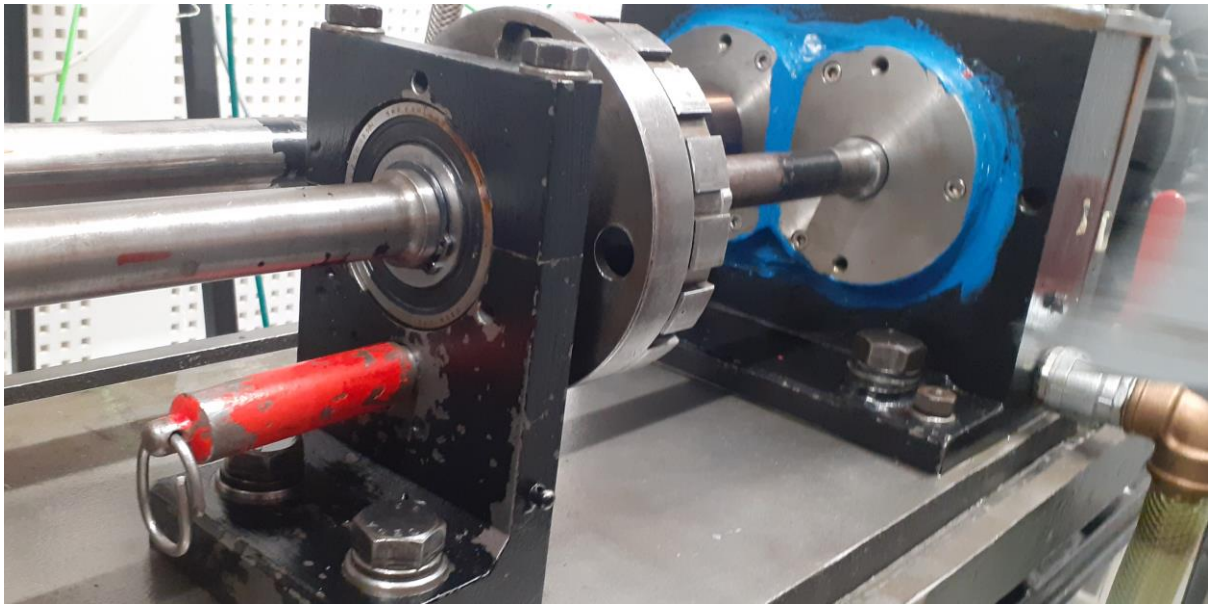

Annexes 2 : Gears parameters calculations

Subscript 1 would refer to the driving gear, subscript 2 would refer to the driven gear.

z: number of teeth

r: pitch radius

r_a: outside radius

m_0: module

h_a: tooth addendum

h_b: tooth dedendum

r_f: root radius

p_b: base pitch

g_f: Length of approach path

g_f: Length of recess path

$$r_a = r + h_a$$

For this gear we assumed that the profile shift coefficient is equal to zero so that $h_a = m_0$

Therefore,

$$r_a = r + h_a$$

$$r_a - m_0 = r$$

$$r_a = m_0 + \left(\frac{m_0 * z}{2}\right)$$

$$r_a = m_0 * \left(1 + \left(\frac{z}{2}\right)\right)$$

Finally,

$$m_0 = r_a * \left(\frac{1}{1 + \frac{z}{2}}\right)$$

Also,

$$h_b = 1.25 * m_0$$

$$r_f = r - 1.25 * m_0$$

$$p_b = 2\pi * (\frac{r_f}{z})$$

$$g_f = \sqrt{{r_{a1}}^2 - {r_1}^2 cos^2\alpha_0} - r_1 sin\alpha_0 \; [m]$$

$$g_a = \sqrt{{r_{a2}}^2 - {r_2}^2 cos^2\alpha_0} - r_2 sin\alpha_0 \; [m]$$

Annexe 3: Torque of the lever calculation

The lever is made of four elements: the white lever and the black, blue and red connectors.

Elements	Mass (g)	CoG (mm)
White lever	3.83	59.6
Black connector	0.52	15.5
Blue connector	0.22	24
Red connector	0.23	113

$$Tl = W * CoG = \sum mg * Cog = 0.0027\ Nm$$

Annexe 4: Torsional analytical model calculation

Circular version

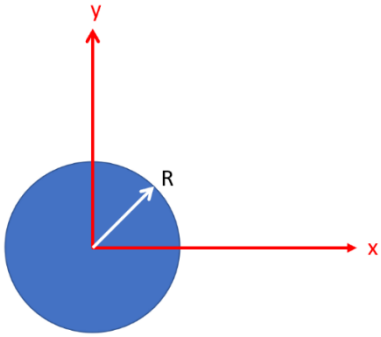

D = 4.72 mm

R= D/2

$$J_z = I_x + I_y$$

$$I_x = I_y = \frac{\pi R^4}{4} = \frac{\pi D^4}{64}$$

$$J_z = 2I_x = \frac{\pi D^4}{32} = 4.8726 * 10^{-11}\ m^4$$

Therefore $\boldsymbol{k = 0.4479\ N/m}$,

Rectangular version

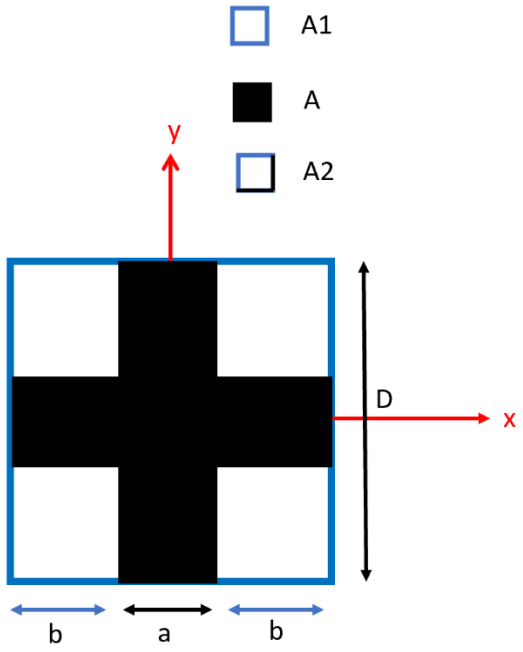

A =A1- 4*A2

a = 1.83mm

b = 1.445mm

A1 = 22.28m^2

A2 = 2.088m^2

D = 4.72mm

R = D/2

$$J_z = I_x + I_y$$

Where, $I_x = I_{x1} - 4I_{x2}$

$$I_{x1} = \iint_{-R}^{R} y^2\, dxdy = \int_{-R}^{R} [y^2 x]dy = \int_{-R}^{R} 2Ry^2 dy = \left[\frac{2Ry^3}{3}\right] = \frac{4}{3}R^4 = \frac{D^4}{12}$$

$$I_{x2} = \iint_{\frac{a}{2}}^{R} y^2\, dxdy = \int_{\frac{a}{2}}^{R} [y^2 x]dy = \int_{\frac{a}{2}}^{R} \left(R - \frac{a}{2}\right) y^2 dy$$

Where $R - \frac{a}{2} = \frac{D}{2} - \frac{a}{2} = b$

$$I_{x2} = \int_{\frac{a}{2}}^{R} y^2 b\, dy = \frac{R^3 - \left(\frac{a}{2}\right)^3}{3} = \frac{b^4}{3}$$

$$J_z = I_x + I_y = 2I_x = 2(I_{x1} - 4I_{x2}) = \frac{1}{6}(D^4 - 16b^4) = 7.1095 * 10^{-11}\, m^4$$

Therefore; $\boldsymbol{k = 0.6534\, N/m}$

<u>Mixed version:</u> the corners of the cross section are cut by the diameter

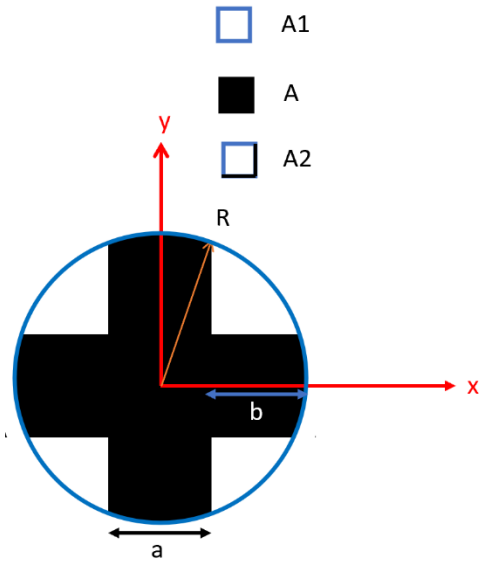

A =A1- 4*A2

a = 1.83mm

b = 1.445mm

A1 = 22.28m^2

A2 = 2.088m^2

D = 4.72mm

R = D/2

$$J_z = I_x + I_y$$

$$I_x = I_y \Rightarrow J_z = 2I_x$$

$$I_x = I_{x1} - 4I_{x2}$$

$$I_{x1} = \frac{\pi D^4}{32}$$

$$I_{x2} = \frac{1}{4}\int_0^{\frac{\pi}{4}}\int_0^{b} R^2\, r dr d\varphi = \int_0^{\frac{\pi}{4}}\left[\frac{R^4}{4}\right] = \frac{1}{4}\frac{\pi b^4}{16}$$

$$J_z = 2(I_{x1} - 4I_{x2}) = \frac{\pi}{32}(D^4 - 4b^4) = 4.7015 * 10^{-11}\, m^4$$

Therefore; $\boldsymbol{k = 0.4321\ N/m}$

Annexe 5: Derivation of induced torque unto system by clutch rotation equation:

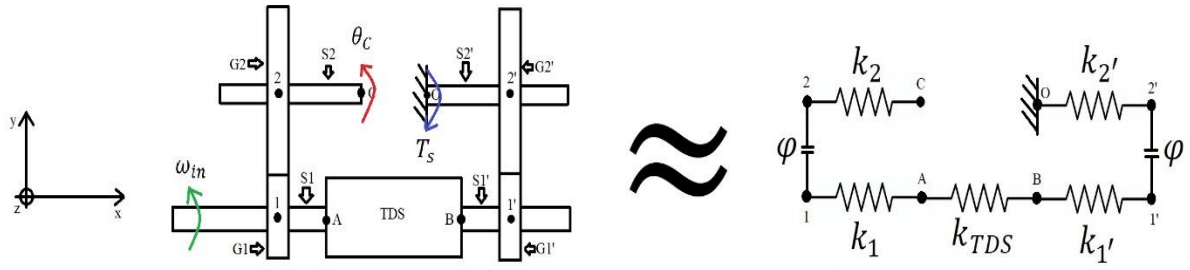

θ: Rotation, ϕ: Angle of twist

Gear ratio:

/G2-G1: $\frac{\theta_2}{\theta_1} = \frac{Z_1}{Z_2} = \varphi$ /G2'-G1': $\frac{\theta_{2'}}{\theta_{1'}} = \frac{Z_{1'}}{Z_{2'}} = \varphi$

Torque ratio:

/G2-G1: $T_1\theta_1 = T_2\theta_2 \rightarrow \frac{T_2}{T_1} = \frac{\theta_1}{\theta_2} = \frac{1}{\varphi}$ /G2'-G1': $T_{1'}\theta_{1'} = T_{2'}\theta_{2'} \rightarrow \frac{T_{2'}}{T_{1'}} = \frac{\theta_{1'}}{\theta_{2'}} = \frac{1}{\varphi}$

Torsional Analysis:

All shafts are in series: $\therefore \phi_C = \phi_{2'} + \phi_{1'} + \phi_{TDS} + \phi_1 + \phi_2$

$$\phi = \int_0^L \frac{T(x)}{J(x)G(x)} \cdot dx$$

$$\phi_C = \frac{T_{2'}L_{2'}}{JG} + \frac{T_{1'}L_{1'}}{JG} + \frac{T_{TDS}L_{TDS}}{3JG} + \frac{T_1L_1}{JG} + \frac{T_2L_2}{JG}$$

/S2': $T_{2'} = T_s$ /S1': $T_{2'}\theta_{2'} = T_{1'}\theta_{1'} \rightarrow T_{1'} = \frac{\theta_{2'}}{\theta_{1'}}T_{2'} = \varphi T_s$

/TDS: $T_{TDS} = T_{1'} = \varphi T_s$ /S1: $T_1 = T_{TDS} = \varphi T_s$

/S2: $T_2\theta_2 = T_1\theta_1 \rightarrow T_2 = \frac{\theta_1}{\theta_2}T_1 = \frac{1}{\varphi}\varphi T_s = T_s$

$$\phi_C = \frac{T_sL_{2'}}{JG} + \frac{\varphi T_sL_{1'}}{JG} + \frac{\varphi T_sL_{TDS}}{3JG} + \frac{\varphi T_sL_1}{JG} + \frac{T_sL_2}{JG}$$

$$\phi_C = T_s\left(\frac{3L_{2'} + 3\varphi L_{1'} + \varphi L_{TDS} + 3\varphi L_1 + 3L_2}{3JG}\right) = T_s\frac{1}{k_{eq}}$$

$$\therefore T_s = k_{eq}\phi_C = \left(\frac{3JG}{3L_{2'} + 3\varphi L_{1'} + \varphi L_{TDS} + 3\varphi L_1 + 3L_2}\right)\phi_C$$

Apparent Angle of Twist analysis:

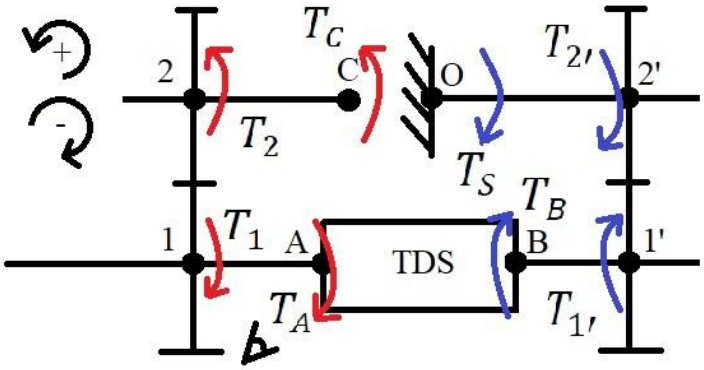

$$T_i = k_i\phi_i, k = \frac{J_i G_i}{L_i}$$

/S2: $T_c = T_2 \qquad \theta_2 = \theta_c$

/S2-S1: $\theta_2 = \varphi\theta_1 \rightarrow \theta_1 = \frac{1}{\varphi}\theta_c,\ T_2\theta_2 = T_1\theta_1 \rightarrow T_1 = \frac{\theta_2}{\theta_1}T_2 = \varphi T_2$

/S1: $T_A = T_1$ /S1-A: $T_2 = k_2\theta_2 \quad T_A = k_1\theta_A \quad T_A = T_1 = \varphi T_2$

$$k_1\theta_A = \varphi\, k_2\theta_2 \rightarrow \theta_A = \varphi\frac{k_2}{k_1}\theta_2 = \varphi\frac{\left(\frac{JG}{L_2}\right)}{\left(\frac{JG}{L_1}\right)}\theta_2 = \varphi\frac{L_1}{L_2}\theta_C$$

/S2'-S1': $\theta_{2'} = \varphi\theta_{1'} \qquad \theta_{2'} = \phi_C$

/S1'-B: $T_{2'} = k_{2'}\theta_{2'} \qquad T_B = k_{1'}\theta_B \qquad T_B = T_{1'} = \varphi T_{2'}$

$$k_{1'}\theta_B = \varphi\, k_{2'}\theta_{2'} \rightarrow \theta_{2'} = \varphi\frac{k_{1'}}{k_{2'}}\theta_B = \frac{1}{\varphi}\frac{\left(\frac{JG}{L_{1'}}\right)}{\left(\frac{JG}{L_{2'}}\right)}\theta_B = \frac{1}{\varphi}\frac{L_{2'}}{L_{1'}}\theta_B$$

/A-B (TDS): $k_{TDS} = \frac{3JG}{L_{TDS}}, \theta_{Tot} = \theta_A + \theta_B$

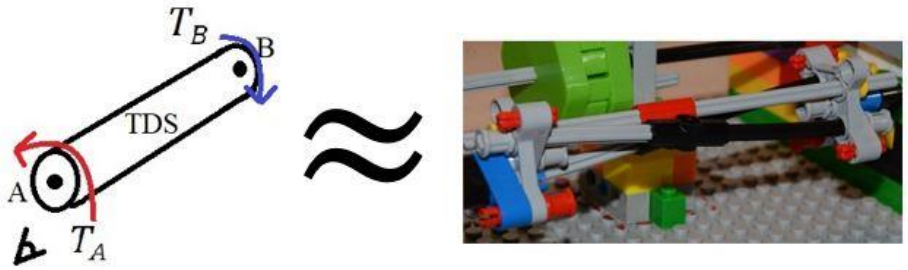

$$\theta_{Tot} = \frac{T_{TDS}}{k_{TDS}}, where\ T_{TDS} = T_A - T_B = k_1\theta_A - k_{1'}\theta_B$$

$$\frac{(T_A - T_B)}{k_{TDS}} = \theta_A + \theta_B \rightarrow k_1\theta_A - k_{1'}\theta_B = k_{TDS}(\theta_A + \theta_B)$$

$$\theta_B(k_{TDS}+k_{1'})=(k_1-k_{TDS})\theta_A \rightarrow \theta_B=\frac{(k_1-k_{TDS})}{(k_{TDS}+k_{1'})}\theta_A$$

$$\theta_B=\frac{\left(\frac{JG}{L_1}-\frac{3JG}{L_{TDS}}\right)}{\left(\frac{3JG}{L_{TDS}}+\frac{JG}{L_{1'}}\right)}\theta_A=\frac{\left(\frac{JG(L_{TDS}-3L_1)}{L_1L_{TDS}}\right)}{\left(\frac{JG(3L_{1'}+L_{TDS})}{L_{TDS}L_{1'}}\right)}\theta_A=\frac{(L_{TDS}-3L_1)L_{TDS}L_{1'}}{L_1L_{TDS}(3L_{1'}+L_{TDS})}\theta_A$$

$$\theta_B=\frac{(L_{TDS}-3L_1)L_{1'}}{(3L_{1'}+L_{TDS})L_1}\theta_A$$

/S1'-S2': $\theta_{2'}=\frac{1}{\varphi}\frac{L_{2'}}{L_{1'}}\theta_B=\frac{1}{\varphi}\frac{L_{2'}}{L_{1'}}\frac{(L_{TDS}-3L_1)L_{1'}}{(3L_{1'}+L_{TDS})L_1}\theta_A$

$$\theta_{2'}=\frac{1}{\varphi}\frac{L_{2'}}{L_{1'}}\frac{(L_{TDS}-3L_1)L_{1'}}{(3L_{1'}+L_{TDS})L_1}\varphi\frac{L_1}{L_2}\theta_C=\frac{L_{2'}(L_{TDS}-3L_1)}{(3L_{1'}+L_{TDS})L_2}\theta_C=\phi_c$$

$$\therefore T_s=k_{eq}\phi_C=\left(\frac{3JG}{3L_{2'}+3\varphi L_{1'}+\varphi L_{TDS}+3\varphi L_1+3L_2}\right)\frac{L_{2'}(L_{TDS}-3L_1)}{(3L_{1'}+L_{TDS})L_2}\theta_C\ [Nm]$$

Annexe 6 :MATLAB code: Analysis.m flow diagrams